

DOT/FAA/AR-99/56

Office of Aviation Research
Washington, D.C. 20591

Solid-State Thermochemistry of Flaming Combustion

Richard E. Lyon

Federal Aviation Administration
Airport and Aircraft Safety
Research and Development Division
William J. Hughes Technical Center
Atlantic City International Airport, NJ 08405

July 1999

Final Report

This document is available to the U.S. public
through the National Technical Information
Service (NTIS), Springfield, Virginia 22161.



U.S. Department of Transportation
Federal Aviation Administration

NOTICE

This document is disseminated under the sponsorship of the U.S. Department of Transportation in the interest of information exchange. The United States Government assumes no liability for the contents or use thereof. The United States Government does not endorse products or manufacturers. Trade or manufacturer's names appear herein solely because they are considered essential to the objective of this report. This document does not constitute FAA certification policy. Consult your local FAA aircraft certification office as to its use.

This report is available at the Federal Aviation Administration William J. Hughes Technical Center's Full-Text Technical Reports page: www.tc.faa.gov/its/act141/reportpage.html in Adobe Acrobat portable document form (PDF).

1. Report No. DOT/FAA/AR-99/56		2. Government Accession No.		3. Recipient's Catalog No.	
4. Title and Subtitle SOLID-STATE THERMOCHEMISTRY OF FLAMING COMBUSTION				5. Report Date July 1999	
				6. Performing Organization Code	
7. Author(s) Richard E. Lyon				8. Performing Organization Report No.	
9. Performing Organization Name and Address Federal Aviation Administration Airport and Aircraft Safety Research and Development Division William J. Hughes Technical Center Atlantic City International Airport, NJ 08405				10. Work Unit No. (TRAIS)	
				11. Contract or Grant No.	
12. Sponsoring Agency Name and Address U.S. Department of Transportation Federal Aviation Administration Office of Aviation Research Washington, DC 20591				13. Type of Report and Period Covered Final Report	
				14. Sponsoring Agency Code AIR-100	
15. Supplementary Notes					
16. Abstract <p>The thermal and chemical processes which occur in the solid state during flaming combustion are examined. A phenomenological model of fuel generation provides the relationships between macroscopic flammability parameters and polymer chemical structure and shows how the coupling of thermal diffusion and chemical kinetics occurs naturally in the pyrolysis zone. Fire behavior and flammability of solid polymers are predicted using the ignition temperature, heat of combustion, heat of gasification, and char yield calculated from the chemical structure; and the results are compared to experimental values. The objective of this work is to develop a consistent, solid-state physical chemistry of flaming combustion which bridges the gap between fire and material sciences to help guide the discovery of new, more fire-resistant polymers.</p>					
17. Key Words Thermochemistry, Combustion, Flammability, Fire, Thermal degradation, Polymers, Char				18. Distribution Statement This document is available to the public through the National Technical Information Service (NTIS), Springfield, Virginia 22161.	
19. Security Classif. (of this report) Unclassified		20. Security Classif. (of this page) Unclassified		21. No. of Pages 61	22. Price

ACKNOWLEDGEMENTS

The author is indebted to Professor James Quintiere for his significant contributions to this manuscript; to Dr. Marc Nyden for his many helpful suggestions; to Richard N. Walters and Dr. Sanjeev Gandhi for experimental support; and to all of the interns, students, post-docs, and editors who conspired to make this work as error free as possible.

TABLE OF CONTENTS

	Page
EXECUTIVE SUMMARY	xi
1. INTRODUCTION	1
2. FIRE BEHAVIOR OF COMBUSTIBLE SOLIDS	3
2.1 Ignition	4
2.2 Steady Burning	5
3. KINETICS	10
3.1 Fuel Generation	10
3.2 Decomposition Temperature	20
4. THERMODYNAMICS	27
4.1 Char Yield	27
4.2 Heat of Gasification	30
4.3 Heat of Combustion	31
4.3.1 Calculation From Oxygen Consumption	34
4.3.2 Calculation From Heats of Formation	35
5. THERMAL-CHEMICAL COUPLING: THE PYROLYSIS ZONE	36
6. CHEMICAL STRUCTURE AND FIRE BEHAVIOR	38
6.1 Flammability	38
6.2 Burning Temperature	39
6.3 Heat Release Rate	40
7. REFERENCES	44

LIST OF FIGURES

Figure		Page
1	Schematic Diagram of Polymer Burning	2
2	Equilibrium Surface Temperature of Polymer Versus External Heat Flux for Fires of Various Sizes	3
3	Geometry of Polymer Combustion Analysis	5
4	Idealized Heat Release Rate Curves for Steady Burning of Noncharring and Charring Polymers	8
5	Net Heat Flux at $\dot{q}_{\text{ext}} = 50 \text{ kW/m}^2$ Versus Polymer Surface Temperature for Emissivities $\epsilon = 0.75$ and 1.0	9
6	Generalized Thermal Degradation Mechanism of Polymers	11
7	Thermogravimetric Scan of Polybenzimidazole at a Linear Heating Rate of 10 K/min Under Nitrogen	11
8	Fire Char Yield Versus Anaerobic Pyrolysis Residue for a Variety of Polymers	13
9	Thermal Degradation Model for Polymers in Fires	13
10	Comparison of Thermal Degradation Model to Nonisothermal TGA Data (Nitrogen Purge) for a Phenolic Triazine Thermoset Polymer	18
11	Peak Mass Loss Temperature Versus Heating Rate for Polymethylmethacrylate (PMMA), Polyethylene (PE), and Phenolic Triazine (PT)	20
12	Calculated Versus Measured Peak Mass Loss Rate in TGA for PMMA, Polyethylene, and Phenolic Triazine at Indicated Heating Rates, $\beta = 1, 3, 5, 10, 20, 30, 100,$ and 200 K/min	20
13	Dependence of Decomposition Temperature on Activation Energy for Pyrolysis	21
14	Peak Pyrolysis Temperature Versus Reciprocal of the Natural Logarithm of the Reduced Heating Rate According to Equation 60	23
15	Relationship Between Limiting Oxygen Index and Char Yield for Halogen (○) and Nonhalogen (●) Polymers From Table 2	28
16	Equilibrium Mass Fraction Versus Temperature for Energy Barriers to Gasification	29
17	Underwriters Laboratory UL 94 Ranking of Flammability Versus the Combined Parameter $\mu+\text{LOI}$ for the Polymers in Table 2 Showing Transition From Burning to Self-Extinguishing Behavior at $\mu+\text{LOI} \approx 0.56$ (56%)	39
18	Surface Temperature of PMMA Versus External Radiant Heat Flux for Steady Nonflaming Gasification	40

19	Average Flaming Heat Release Rate Versus Char Yield for Polymers Listed in Table 2	41
----	--	----

LIST OF TABLES

Table		Page
1	Group Contributions to the Decomposition Temperature of Polybenzimidazole after Van Krevelen	25
2	Peak Pyrolysis Temperature (T_p), Pyrolysis Residue (μ), Limiting Oxygen Index (LOI), and UL 94 Ranking of Some Polymers	26
3	Group Contributions to the Char Residue of Poly(etheretherketone) From Reference 93	29
4	Enthalpies of Gasification for PMMA, PS, and PE	30
5	Heats of Gasification, Pyrolysis Activation Energy, Char Yield, and Calculated Molecular Weight of Decomposition Products for Some Polymers Listed in Table 2	32
6	Measured and Calculated Gross Heats (Q_c) of Polymer Combustion	33
7	Group Contributions to the Heat of Formation of PMMA	35

LIST OF SYMBOLS

α	= Thermal diffusivity ($\approx 10^{-7}$ m ² /s for polymers)
A	= Frequency factor for pyrolysis (sec ⁻¹)
A_g	= Frequency factor for gas generation (sec ⁻¹)
A_c	= Frequency factor for char formation (sec ⁻¹)
b	= Sample thickness
β	= Linear (constant) heating rate (K/s)
χ	= Gas phase combustion efficiency (dimensionless)
C	= Molar heat capacity (J/mol-K)
c	= Heat capacity (J/g-K)
δ	= Pyrolysis zone depth (m)
e	= the natural number 2.718...
ϵ	= Surface emissivity of radiant energy (dimensionless)
E	= Energy released by combustion per mass of oxygen consumed = 13.1 kJ/g-O ₂
E_a	= Activation energy for pyrolysis (J/mol)
E_g	= Activation energy for gas formation (J/mol)
E_c	= Activation energy for char formation (J/mol)
ΔG^*	= Free Energy of Activation for Pyrolysis (J/mol)
\bar{h}	= Average surface convective heat transfer coefficient (W/m ² -K)
h_c°	= Net heat of complete combustion of polymer pyrolysis gases (J/kg)
$h_{c,\mu}^\circ$	= Net heat of complete combustion of polymer char (J/kg)
$h_{c,p}^\circ$	= Net heat of complete combustion of solid polymer (J/kg)
h_g	= Heat of polymer gasification (J/kg)
ΔH_c	= Molar enthalpy of complete combustion (J/mol)
ΔH_g	= Molar enthalpy of gasification (J/mol)
ΔH_d	= Molar enthalpy of primary bond dissociation (J/mol)
ΔH_f	= Molar enthalpy of fusion (J/mol)
ΔH_s	= Stored molar enthalpy (J/mol)
ΔH_v	= Molar enthalpy of vaporization (J/mol)
ΔH^*	= Activation enthalpy for pyrolysis
η_c	= Kinetic heat release capacity (J/g-K)
I*	= Reactive intermediate for pyrolysis
k_p	= Global Arrhenius rate constant for pyrolysis (sec ⁻¹)
k_g	= Arrhenius rate constant for gas generation (sec ⁻¹)
k_c	= Arrhenius rate constant for char formation (sec ⁻¹)
k_i	= Arrhenius rate constant for initiation of bond breaking (sec ⁻¹)
k_r	= Arrhenius rate constant for bond recombination (sec ⁻¹)
κ	= Thermal conductivity (W/m-K)
m	= Instantaneous sample mass (kg)
m_o	= Initial sample mass (kg)
\dot{m}_{max}	= Peak mass loss rate (kg/s)
μ	= Char yield or pyrolysis residue of polymer at 850°C (g/g)
M_g	= molecular weight of gaseous decomposition species (g/mol)
M	= monomer molecular weight (g/mol)
N	= Number of collisions with energy E_a at the peak pyrolysis temperature T_p .
\dot{Q}_c	= Kinetic heat release rate (W/kg)

\dot{q}_c	=	Average or steady-state heat release rate in a bench scale test (kW/m ²)
\dot{q}_{cr}	=	Critical heat flux for ignition (kW/m ²)
\dot{q}_{ext}	=	External heat flux in a fire or test (kW/m ²)
\dot{q}_{net}	=	Net heat flux to the surface of a burning sample (W/m ²)
\dot{q}_{flame}	=	Flame heat flux (W/m ²)
ρ	=	Polymer density (kg/m ³)
r	=	Mass loss rate exponent $(1+2RT_p/E_a)^{-1}$ (dimensionless)
R	=	Ideal gas constant (= 8.314 J/mol-K)
σ	=	Boltzmann radiation constant = 5.7×10^{-8} W/m ² -K ⁴
S	=	Surface area (m ²)
ΔS^*	=	Molar activation entropy for pyrolysis (J/mol)
t	=	Time (s)
T_p	=	Temperature at peak pyrolysis rate in linear heating program (K)
T_s	=	Sample or surface temperature (K)
T_o	=	Ambient (room) temperature (K)
$T_{d,1/2}$	=	Temperature at 50% of ultimate weight loss (K)
$T_{d,0}$	=	Temperature of initial weight loss (K)
$T_{d,max}$	=	Temperature at maximum rate of weight loss during slow heating (K)
v	=	Surface regression rate at steady state burning (m/s)
V	=	Volume (m ³)
Y_c	=	Temperature-dependent equilibrium residual mass fraction (dimensionless)
Z	=	Zip length for thermal degradation by end chain scission.

EXECUTIVE SUMMARY

A self-consistent materials chemistry of flaming combustion is derived from solid-state kinetics and thermodynamics using a realistic physical model of polymer burning. The rates of solid-state (pyrolysis) and gas phase (combustion) reactions are assumed to be rapid in comparison to the rate of heat transfer at the burning surface. Coupling of thermal diffusion and chemical kinetics occurs in the surface pyrolysis zone where the rate of temperature rise for steady burning becomes the characteristic heating rate for thermal decomposition.

Detailed thermal degradation chemistry is foregone in favor of a transient mass balance on the polymer, fuel gases, and solid char in the anaerobic pyrolysis zone. Closed-form, time-independent solutions for the scalar mass loss rate and char yield are obtained from the degradation kinetics which, in combination with the solid-state thermal transport and thermodynamic properties calculated from the polymer chemical structure, provide the scaling relationship between material properties and steady-burning rate. The critical condition for a nonzero burning rate in the absence of an external heat flux (flammability) can then be expressed in terms of material properties.

Thermochemical predictions of ignitability and flaming heat release rate for a variety of charring and noncharring polymers are in general agreement with experimental data using the present approach.

1. INTRODUCTION.

Synthetic polymers have improved our quality of life since their commercial introduction over 50 years ago. Synthetic polymers can be low-cost functional replacements for metals or natural polymers (e.g., wool, silk, leather, and wood) with improved physical, chemical, and optical properties or can be enabling materials for high-technology applications such as electronics, optics, medical devices, and aerospace. Commodity applications of synthetic polymers include home furnishings, appliances, construction, recreation, and consumer packaging; but it is the performance-critical, high-technology applications that have driven the development of thermally and chemically stable polymers with intrinsic fire resistance [1, 2, 3, 4, 5, 6, 7, 8, 9, 10, 11, 12].

The use of polymers in public buildings and mass transportation where fire is a significant threat to human life because of the potential for rapid fire spread calls for a balance between the functionality of polymers and their risk as a fire hazard. Flames from fires destroy property, but it is the combustion products in the smoke which, directly or indirectly, lead to loss of life [13, 14, 15]. Conventional methods of reducing ignitability in small flame tests by the addition of flame-retarding chemicals usually increases the density and toxicity of smoke and fumes [13, 16]. Although flame-retardant materials may burn less vigorously under real fire conditions [16], the lowered burn rate is usually accompanied by higher smoke levels resulting from incomplete gas phase combustion. Incomplete combustion increases the carbon monoxide/carbon dioxide ratio and the toxic potency of the smoke [14, 16]. Thus, the most effective way to improve the fire safety of components is to use intrinsically fire-resistant polymeric materials [17, 18, 19] with reduced burning rate and high gas phase combustion efficiency.

The above and subsequent references to polymer burning are understood to mean the gas phase combustion of the mixture of oxygen and polymer thermal degradation products in a fire, since technically polymers do not burn in the condensed (solid or liquid) state. Polymers do not burn in the condensed state because of the low solubility and diffusivity of the oxidizer (diatomic oxygen) and the low oxidation rate at the decomposition temperature. In fact, thermal degradation of the surface layer of polymer in the presence of a heat source is thought to occur in a reducing, rather than an oxidizing, environment. Low molecular weight volatile organic compounds are produced which mix with atmospheric oxygen above the polymer surface to form a flammable mixture which when ignited combusts, producing a luminous flame. Of particular interest is the rate of fuel generation at the polymer surface in a fire since this process governs the heat release rate and smoke evolution during gas phase combustion.

Figure 1 illustrates the three coupled processes required for flaming combustion: (1) heating of the polymer, (2) thermal decomposition to gaseous products, and (3) ignition and combustion in air. An ignition source or thermal feedback of radiant energy from the flame supplies heat to the polymer surface which causes thermolytic cleavage of primary chemical bonds in the polymer molecules. Evaporation of the low molecular weight degradation products and reaction with air (oxygen) in the combustion zone above the surface releases heat and produces carbon dioxide, water, and incomplete combustion products such as carbon monoxide, unburned hydrocarbons, and soot. In order to resist burning, the fire cycle must be broken at one or more places.

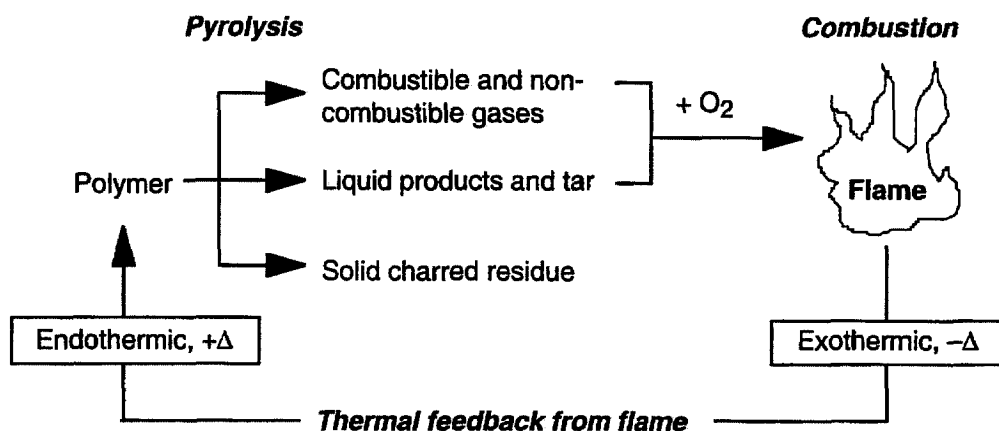


FIGURE 1. SCHEMATIC DIAGRAM OF POLYMER BURNING

Whether a polymer is fire resistant or contributes to the spread of fire depends on the intensity of the fire or heat source and the polymer's reaction to it (e.g., fuel generation rate). Heat fluxes range in intensity from a small ignition source such as a match or cigarette (≈ 20 W), to a Bunsen burner flame ($\approx 10^2$ W), to a trash can fire ($\approx 10^5$ W), to a full-sized room fire ($\approx 10^6$ W), and to a building or hydrocarbon pool fire ($\approx 10^7$ W) [20, 21]. Surprisingly, the heat flux, which is the rate at which heat enters per unit area of an adjacent material surface, falls into the relatively narrow range [20] of 20–200 kW/m² for this 10^7 range of fire sizes. It is the area of the heated surface, not the heat flux itself, which is proportional to the fire size [20].

Figure 2 shows the maximum possible surface temperature for an $\epsilon = 0.75$ emissivity material as a function of incident heat flux for a surface convective heat transfer coefficient $\bar{h} = 15$ W/m²-K assuming thermal equilibrium [22]

$$\dot{q}_{\text{ext}} = \epsilon\sigma[T_s^4 - T_o^4] + \bar{h}[T_s - T_o] \quad (1)$$

Ranges of heat flux incident on a material in proximity to fires of different sizes are shown parallel to the horizontal (heat flux) axis in figure 2. The vertical axis is subdivided into qualitative fire performance rankings which presume short-term thermal stability (decomposition temperature) in the range of surface temperatures experienced by a material in various fire environments. Small diffusion flames of burning material have heat fluxes in the range of 25-40 kW/m² corresponding to the range of sample surface temperatures 500-600°C in figure 2. Polymers with short-term thermal stability in this range of temperatures are typically flame resistant since they will not continue to burn in the absence of an external heat source or elevated oxygen concentration. Small fires in proximity to the polymer surface (e.g., a burning wastebasket) or remote large fires generate surface heat fluxes in the range 30-60 kW/m² depending on their size and distance from the surface. Heat fluxes of 30-60 kW/m² generate equilibrium surface temperatures in the 550–750°C range. Polymers with short-term thermal stability in this range of temperatures may be categorized as fire resistant since they typically resist piloted ignition or, when ignited, burn with a low rate of heat release (≤ 100 kW/m²). Intrinsically fire-resistant polymers are thermally stable polycyclic and heteroatomic molecules with low hydrogen content. Noncombustible behavior in figure 2 and in standard tests [23] are associated with short-term thermal stability at or above temperatures of 750°C, corresponding to heat fluxes in excess of 75 kW/m² in figure 2. These large heat fluxes result from contact with, or close proximity to, fully developed large fires such as liquid

hydrocarbon pool fires, burning buildings, or post-flashover compartments. Noncombustible materials are presently inorganic in composition [24].

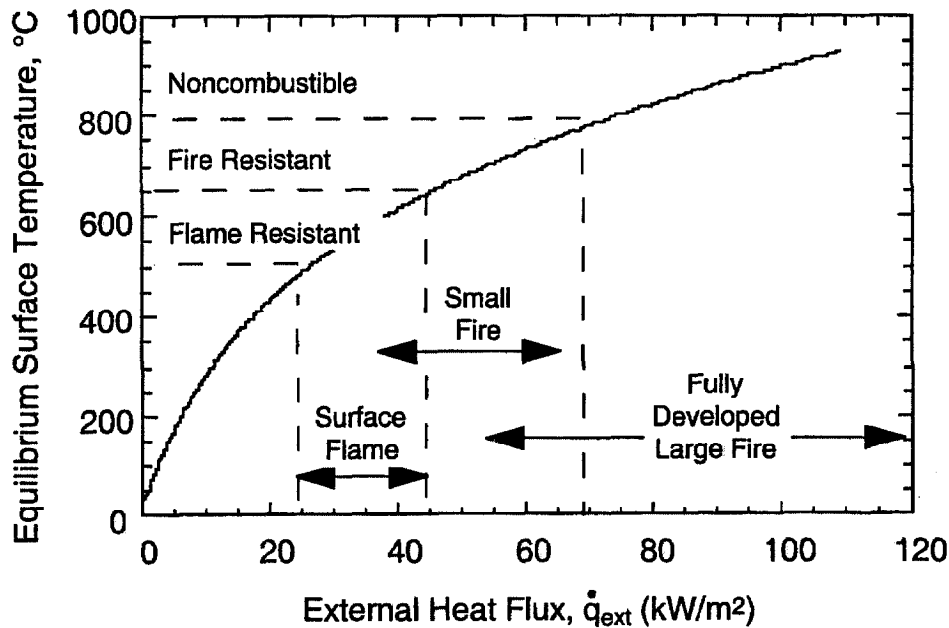


FIGURE 2. EQUILIBRIUM SURFACE TEMPERATURE OF POLYMER VERSUS EXTERNAL HEAT FLUX FOR FIRES OF VARIOUS SIZES

Several comprehensive texts have been written on the gas phase processes of flaming combustion [25, 26, 27, 28] while the thermochemical processes which occur in the solid state to generate the combustible gases in a fire have received relatively little attention [29, 30]. The remainder of this chapter explores the material science of flaming combustion by developing relationships between the chemical structure of polymers and their burning behavior. Recent developments in the metrology and modeling of fire [31, 32] and its impact on materials [29, 33, 34, 35] provide a physical basis for polymer ignition and burning in terms of measurable, macroscopic flammability parameters. Connecting these macroscopic flammability parameters to the molecular structure of the polymer through the kinetics and thermodynamics of the fuel generation process provides a thermochemical basis for the solid-state processes of flaming combustion.

2. FIRE BEHAVIOR OF COMBUSTIBLE SOLIDS.

The solid-state processes in the flaming combustion of polymers which can be treated at the continuum level are the subject of this section. The continuum treatment disregards the discrete (molecular) structure of matter so that the temperature distribution and more importantly its derivatives are continuous throughout the material. In addition, the material is assumed to have identical thermal properties at all points (homogeneous) and in all directions (isotropic). The concept of a continuous medium allows us to define fluxes at a point, e.g., a surface in one-dimensional space. Chemical reactions in the solid (pyrolysis) and flame (combustion) are assumed to occur so rapidly that the burning rate is determined solely by the heat transfer rate [26]. Differential [36, 37, 38, 39] and integral [40, 41] condensed-phase burning models have been developed from the continuum perspective with coupled heat and mass transfer for both charring [36, 37, 40] and noncharring polymers [39, 41]. All of these models must be solved numerically for the transient (time-dependent) mass loss and heat release rates.

In the present treatment we neglect transient phenomena in thick samples, such as char layer growth and the progression of crystalline melting, and consider only the quasi-steady burning of an idealized solid with constant surface heat flux. This simplified approach allows us to develop algebraic (scaling) relationships between material composition and the solid-state processes of flaming combustion but ignores many important details of thick-sample burning behavior which can only be captured through transient numerical analysis.

2.1 IGNITION.

Figure 3 shows the geometry of the continuum model of polymer combustion. If the polymer thickness $b+\delta$ in figure 3 is large compared to the thermal degradation process (pyrolysis) zone thickness δ (i.e., $b \gg \delta$), then according to the critical surface temperature criteria for ignition, sustained piloted ignition occurs when the polymer surface reaches its thermal decomposition temperature. A critical surface temperature is only one of several criteria which have been proposed for ignition [42]. Other critical values at ignition include the average temperature of the solid, pyrolyzate mass flux, char depth, rate of increase of local gas temperature, reaction rate in the gas boundary layer, and a gas temperature gradient reversal. As will be shown in the following sections, the decomposition temperature of a polymer is a kinetic parameter whose exact value depends on the heating rate (heat flux).

Heat transfer in the solid polymer is described by the one-dimensional energy equation for unsteady heat conduction with no internal heat generation

$$\frac{\partial T}{\partial t} - v \frac{\partial T}{\partial x} = \alpha \frac{\partial^2 T}{\partial x^2} \quad (2)$$

where T is the temperature at location x in the solid polymer and $\alpha = \kappa/\rho c$ is the polymer thermal diffusivity in terms of its thermal conductivity, κ , density, ρ , and heat capacity, c ; and v is the regression velocity of the burning surface. During the preheat phase prior to ignition, there is no surface regression, so $v = 0$ and equation 2 reduces to

$$\frac{\partial^2 T}{\partial x^2} - \frac{1}{\alpha} \frac{\partial T}{\partial t} = 0 \quad (3)$$

The solution [43] of equation 3 for the ignition time t_{ign} of a thermally thick sample with a constant net heat flux \dot{q}_{net} at the surface $x = 0$ is

$$t_{\text{ign}} = \frac{\pi}{4} \kappa \rho c \left[\frac{T_{\text{ign}} - T_o}{\dot{q}_{\text{net}}} \right]^2 \quad (4)$$

where T_{ign} is the (piloted) ignition temperature which is approximately equal to the peak mass loss temperature T_p for transient heating [44], and T_o is the ambient initial temperature. If δ is greater than the sample thickness the sample is considered thermally thin, and ignition occurs at time

$$t_{\text{ign}} = \rho b c \left[\frac{T_{\text{ign}} - T_o}{\dot{q}_{\text{net}}} \right] \quad (5)$$

Equations 4 and 5 state that the time to ignition is determined by the ignition (decomposition) temperature; the material's thermal and transport properties κ , ρ , and c ; and the net heat flux to the

surface. Equations 4 and 5 are accurate when the incident heat flux is high compared to heat losses by surface convection and reradiation.

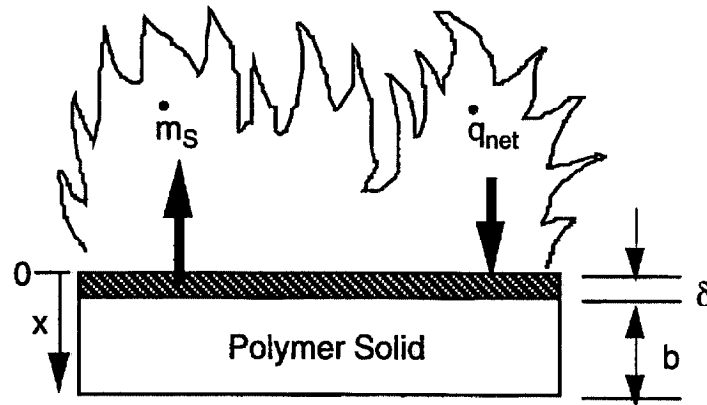


FIGURE 3. GEOMETRY OF POLYMER COMBUSTION ANALYSIS

2.2 STEADY BURNING.

Once sustainable ignition has occurred, steady, one-dimensional burning of the polymer is assumed. Steady burning at a constant surface heat flux is treated as a stationary state by choosing a coordinate system which is fixed to the surface and moving at the recession velocity v . If there is no internal heat generation or absorption, the one-dimensional heat conduction equation (equation 2) applies. Since semicrystalline polymers absorb the heat of fusion during melting at temperatures below the decomposition temperature, equation 2 is only approximate for these materials. Under steady-state conditions, $dT(x)/dt = 0$ and the constant thickness pyrolysis zone moves through the infinitely thick solid with a fixed temperature gradient so that equation 2 becomes

$$\frac{d^2T}{dx^2} + \frac{v}{\alpha} \frac{dT}{dx} = 0 \quad (6)$$

for steady burning of a material with a constant thermal diffusivity $\alpha = \kappa/\rho c$. The general solution of equation 6 is

$$T(x) = c_1 + c_2 \exp[-vx/\alpha] \quad (7)$$

Two boundary conditions are needed to evaluate the constants of integration c_1 and c_2 in equation 7. Conservation of energy at the pyrolysis front $x = 0$ gives

$$\kappa \left. \frac{dT(x)}{dx} \right|_{x=0} = -\dot{q}_{net} + \rho v \Delta h_v = -c_2 \frac{\kappa v}{\alpha} \quad (8)$$

from which $c_2 = (\dot{q}_{net} \alpha/\kappa v) - (\Delta h_v/c)$ with Δh_v the latent heat of vaporization of the pyrolysis products and \dot{q}_{net} the net heat flux at the surface ($x = 0$) expressed as

$$\begin{aligned}\dot{q}_{\text{net}} &= \dot{q}_{\text{ext}} + \dot{q}_{\text{flame}} - \varepsilon\sigma(T_s^4 - T_o^4) - \bar{h}(T_s - T_o) \\ &= \dot{q}_{\text{ext}} + \dot{q}_{\text{flame}} - \dot{q}_{\text{cr}}\end{aligned}\quad (9)$$

Equation 9 defines the net heat flux into the surface \dot{q}_{net} as the difference between the heat flux entering the surface from an external radiant energy source, \dot{q}_{ext} , and/or surface flame, \dot{q}_{flame} , and the critical heat flux for ignition, \dot{q}_{cr} . The critical heat flux for ignition is equal to the heat removed by reradiation, $\varepsilon\sigma(T_s^4 - T_o^4)$, and convection, $h(T_s - T_o)$, at the ignition temperature $T_s = T_{\text{ign}} = T_p$ where ε , σ , and h are the surface emissivity, Stefan-Boltzmann constant, and average surface convective heat transfer coefficient, respectively. In the absence of an external radiant energy source (e.g., during a Bunsen burner-type flammability test), $\dot{q}_{\text{net}} = 0$ when $\dot{q}_{\text{cr}} = \dot{q}_{\text{flame}}$.

On the rear face of the infinite slab ($x = \infty$), we specify $dT/dx = 0$ or equivalently $T(\infty) = T_o = c_1$ where T_o is the ambient temperature in equation 8. The final temperature distribution during steady-state burning of an infinitely thick material is

$$T(x) = T_o + \frac{\dot{q}_{\text{net}}}{\rho c} \frac{1}{v} \exp\left[-\frac{v}{\alpha}x\right] \quad (10)$$

The steady recession velocity of the surface $x = 0$ at temperature $T(0) = T_p$ from equation 10 is

$$v = \frac{1}{\rho} \frac{\dot{q}_{\text{net}}}{\left(c(T_p - T_o) + \Delta h_v\right)} = \frac{1}{\rho} \frac{\dot{q}_{\text{net}}}{h_g} \quad (11)$$

where the total heat of gasification h_g per unit original mass of polymer is [45]

$$h_g = c(T_p - T_o) + \Delta h_v. \quad (12)$$

Equations 10 and 11 allow the steady-state temperature distribution in the burning solid polymer to be expressed as

$$T(x) - T_o = (T_p - T_o) \exp\left(-\frac{c \dot{q}_{\text{net}}}{\kappa h_g} x\right)$$

which is in qualitative agreement with experimental data for the temperature gradient in steadily burning liquid pools [32] if T_p is taken as the boiling temperature of the liquid fuel.

Conservation of mass for the control volume in which the virgin polymer of density ρ pyrolyzes to an inert fraction or char residue μ gives (personal communication, J. Quintiere, University of Maryland, 1999).

$$\rho v = \frac{\dot{m}_g}{1 - \mu} \quad (13)$$

where \dot{m}_g is the mass loss rate of pyrolysis gases per unit surface area. Defining a heat of gasification per unit mass of volatiles

$$L_g = \frac{h_g}{1 - \mu}$$

and combining equations 11 and 13

$$\dot{m}_g = \frac{\dot{q}_{net}}{h_g/(1 - \mu)} = \frac{\dot{q}_{net}}{L_g} \quad (14)$$

The heat of gasification per unit mass of solid polymer h_g can be determined from the reciprocal slope of a plot of areal mass loss rate *versus* external heat flux if the char yield is measured after the test, since from equations 9 and 13

$$\dot{m}_g = \frac{\dot{q}_{ext}}{L_g} - \left(\frac{\dot{q}_{flame} - \dot{q}_{cr}}{L_g} \right) \quad (15)$$

The reciprocal slope of \dot{m}_g *versus* \dot{q}_{ext} equals L_g only if \dot{q}_{flame} does not change with \dot{q}_{ext} or if $\dot{q}_{flame} \ll \dot{q}_{ext}$. Multiplying equation 15 by the net chemical heat of complete combustion of the volatile polymer decomposition products h_c° and the gas phase combustion efficiency χ (see section 4.3) gives the usual result for the average heat release rate of a burning specimen [32, 46].

$$\dot{q}_c = \chi h_c^\circ \dot{m}_g = \chi (1 - \mu) \frac{h_c^\circ}{h_g} \dot{q}_{net} = \chi \frac{h_c^\circ}{L_g} \dot{q}_{net} \quad (16)$$

Given that χ lies in the relatively narrow range [46], $\chi = 0.5-0.9$, it is the combustibility ratio [47] or heat release parameter [46] $h_c^\circ/L_g = (1-\mu)/h_g$ which is the dominant material burning parameter since it can vary by more than an order of magnitude for polymer solids [46]. Since h_g is relatively constant for a wide range of materials (sections 4.2 and 4.3), it is the variation in char yield $\mu = 0 - 0.8$ and $h_c^\circ = 3 - 45$ kJ/g which accounts for most of the difference in the heat release parameter between materials.

Figure 4 shows idealized heat release rate histories for steady burning of thermally thick polymers according to the equations developed in this section. The upper curves represent steady burning of a noncharring ($\mu = 0$) and charring ($\mu \approx 0.5$) polymer, respectively, with comparable h_g . The time-independent heat release rate curve for the charring material (dashed line) is hypothetical since the steady-burning model assumes a constant surface recession rate, i.e., no accumulation of char at the surface. The lower curve (solid line) is a realistic heat release history for a charring polymer showing transient effects such as a peak in heat release rate soon after ignition followed by a depression in the heat release rate as the char layer increases in thickness. The growing char layer insulates the underlying polymer from the surface heat flux and acts as a diffusion barrier to the volatile fuel. Charring polymers can be linear (thermoplastic) or crosslinked (thermoset) polymers having amorphous or semicrystalline morphologies. The area under the heat release rate curves per unit mass of polymer consumed is the effective heat of flaming combustion. The effective heat of combustion is determined primarily by the combustion chemistry in the flame. Combustion efficiency decreases when halogens are present, when soot/smoke is produced in large yield, or when there is insufficient oxygen for complete combustion. Flaming combustion efficiency is relatively independent of the charring tendency of a polymer.

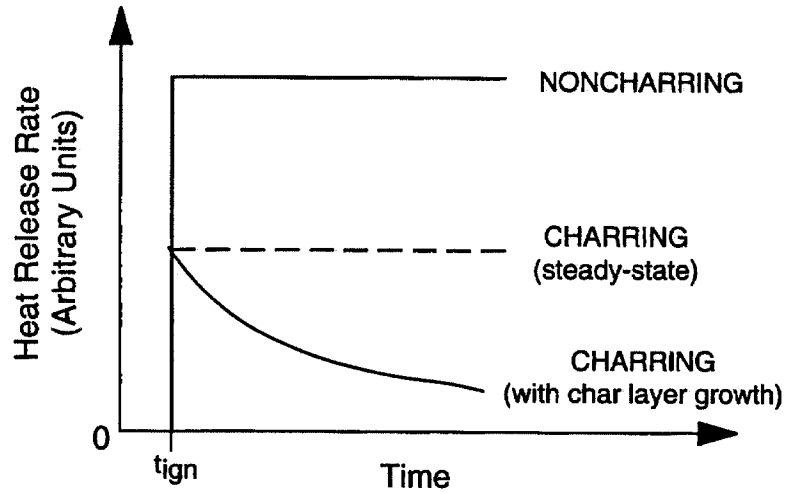


FIGURE 4. IDEALIZED HEAT RELEASE RATE CURVES FOR STEADY BURNING OF NONCHARRING (TOP) AND CHARRING (MIDDLE) POLYMERS (The lower curve is the actual behavior of charring polymers.)

In the subsequent development of the fuel generation rate using thermal degradation kinetics, it will be useful to know the rate of temperature rise of the polymer surface in the pyrolysis zone as it moves through the solid at constant velocity, v . From equations 10 and 11 the effective heating rate at the surface is

$$\left. \frac{dT}{dt} \right|_{x=0} = v \left. \frac{dT}{dx} \right|_{x=0} = \frac{\dot{q}_{net}^2}{\kappa \rho c (T_p - T_o)} \left(1 + \frac{\Delta h_v}{c(T_p - T_o)} \right)^{-2} \quad (17a)$$

Typically, $\Delta h_v/c(T_p - T_o) \approx 0.4 \pm 0.1$ (see section 4.2) so the heating rate at the surface is approximately

$$\left. \frac{dT}{dt} \right|_{x=0} \approx \frac{1}{2} \frac{\dot{q}_{net}^2}{\kappa \rho c (T_p - T_o)} \approx \frac{\dot{q}_{net}^2}{\kappa \rho h_g} \quad (17b)$$

According to equation 17b the rate of surface temperature rise of a polymer with $T_p \approx 500^\circ\text{C}$ (723 K) and a typical $\kappa \rho c = 5 \times 10^5 \text{ W-s-m}^{-4}\text{-K}^{-2}$ experiencing a 50 kW/m^2 net surface heat flux is $dT/dt = 5 \text{ K/s}$.

Figure 5 is a plot of net heat flux versus surface temperature for polymers at an external heat flux $\dot{q}_{ext} = 50 \text{ kW/m}^2$ calculated from equations 9 and 16. Plotted in figure 5 is the calculated net heat flux *versus* surface temperature curves for a horizontal plate with an average surface free convective heat transfer coefficient, $h = 15 \text{ W/m}^2\text{-K}$, for polymer emissivities $\epsilon = 0.75$ and 1.0 . Calculations such as those plotted in figure 5 can be used to determine the ignitability and heat release rate of a polymer as follows. The minimum (net) heat flux for ignition can be calculated using the criteria that ignition occurs when the mass flux exceeds the critical value $\dot{m}_g \approx 3\text{-}5 \text{ g-m}^{-2}\text{-s}^{-1}$ [42]. For typical values $\chi = 0.8$ and $h_c^\circ = 30 \text{ kJ-g}^{-1}$, the critical mass flux corresponds to a critical heat release $\dot{q}_{c,cr} = \chi h_c^\circ \dot{m}_g \approx 100 \text{ kW/m}^2$ (46).

Setting $\dot{q}_c = 100 \text{ kW/m}^2$ in equation 16, the critical net heat flux for ignition of a noncharring polymer with typical $h_g = L_g = 3 \text{ kJ/g}$ is

$$\dot{q}_{\text{net, cr}} = \frac{100 \text{ kW/m}^2}{\chi h_c^\circ / L_g} \approx \frac{100 \text{ kW/m}^2}{(0.8)(30 \text{ kJ/g}) / (3 \text{ kJ/g})} \approx 13 \text{ kW/m}^2$$

which is in the range $\dot{q}_{\text{net, cr}} = 10\text{-}15 \text{ kW/m}^2$ measured for nonhalogen commodity polymers [46]. Figure 5 shows that polymers which can sustain surface temperatures in the range 600-650°C without thermally degrading to gaseous fuel are able to reradiate and convect away enough heat at $\dot{q}_{\text{ext}} = 50 \text{ kW/m}^2$ to ensure that the absorbed (net) heat flux is below the critical value for ignition indicated by the dashed line. This result is in agreement with experimental data for the thermally stable benzobisoxazole polymer [48] which decomposes at temperatures above 650°C and is thus able to resist ignition at $\dot{q}_{\text{ext}} = 50 \text{ kW/m}^2$. Figure 5 also shows that the emissivity of the polymer surface has a significant effect on the net heat flux into the solid. Low-emissivity (heat reflective) coatings are used commercially for ignition-resistant firefighting apparel, paints, and aircraft evacuation slides.

Improved ignition resistance can also be achieved by reducing the magnitude of the quantity $\chi h_c^\circ / L_g$ so that the critical heat flux for ignition increases. Polymer formulators use this strategy to pass small-scale flame resistance tests using chemical flame-retardant additives [49]. Halogenated compounds are routinely added to polymers to interrupt the gas phase combustion process and reduce χ . Metal hydrates which decompose endothermically to inert gases (e.g., H_2O) when heated are added to dilute the combustibles in the solid and in the flame [50]. Inert compounds and char promoters increase L_g by allowing the polymer to absorb heat without liberating fuel. Some flame-retardant additives work by a combination of mechanisms (i.e., synergistically), but the overall effect is to elevate the critical heat flux for ignition in the flame test until the flame retardant is depleted from the polymer.

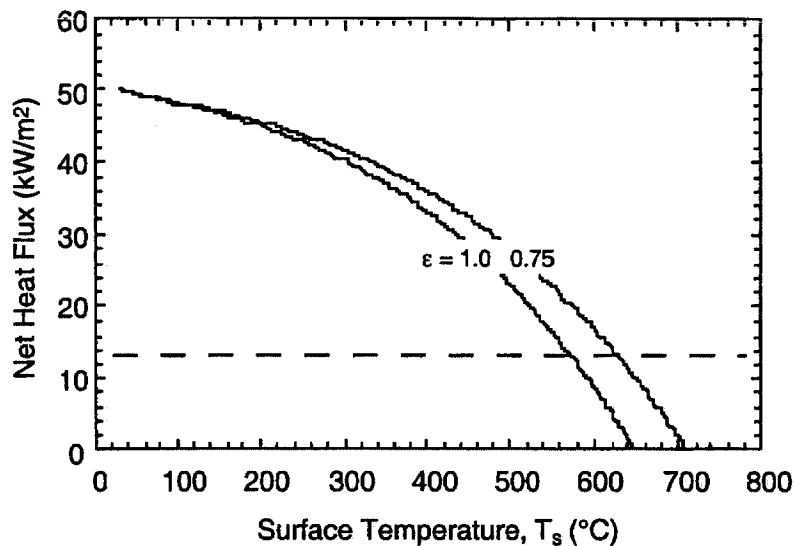


FIGURE 5. NET HEAT FLUX AT $\dot{q}_{\text{ext}} = 50 \text{ kW/m}^2$ VERSUS POLYMER SURFACE TEMPERATURE FOR EMISSIVITIES $\epsilon = 0.75$ and 1.0 (Dashed line is the critical heat flux for $\chi h_c^\circ / L_g = 8$.)

The continuum analyses demonstrated the critical parameters for fire-resistant/low heat release rate polymers: high decomposition temperature T_p , low fuel value of degradation products h_c° , a large heat of gasification h_g , and high char yield μ . While low combustion efficiency χ is a viable route to ignition-resistant materials, the increased hazard associated with higher smoke and fumes from flame-retarded materials in well developed fires argues against this mechanism of fire resistance. In the following sections we explore the molecular basis for the macroscopic fire parameters in an effort to make quantitative predictions about the fire resistance of a polymer from its chemical structure.

3. KINETICS.

The continuum level treatment in the previous section shows that a high decomposition temperature delays ignition (equation 3) and lowers heat release rate (equations 13 and 16) by increasing the stored heat at polymer gasification. Charring is a solid phase mechanism of fire resistance which limits the amount of combustibles which can be generated during thermal degradation and burning. In this section we provide a mechanism for fuel generation in charring and noncharring polymers using thermal degradation kinetics and show that the pyrolysis temperature is essentially a kinetic parameter.

The elementary fuel generation step is thermal degradation of the polymer [49, 51]. Typically, it is the low fraction and rate of production of volatile fuel at fire temperatures and the low heat of combustion of this fuel which make polymers intrinsically fire resistant. Short-term thermal stability and reduced fuel fraction (increased char yield) are achieved by eliminating hydrogen atoms from the polymer molecule so that recombination of carbon radicals to form char during thermal degradation is kinetically favored over hydrogen abstraction/termination reactions which produce volatile fuel fragments [52, 53]. A low heat of combustion of the volatile thermal decomposition products is achieved by substituting heteroatoms (e.g., halogens, nitrogen, phosphorus, sulfur, silicon, boron, and oxygen) for carbon and hydrogen in the polymer molecule. Heteroatoms form stable gas phase combustion products which are either low in fuel value (i.e., N_2 , SO_2 , hydrogen halides) or thermally stable solid oxides (i.e., SiO_2 , P_2O_5 , B_2O_3) which precipitate onto the polymer surface and act as mass- and thermal-diffusion barriers [49, 50].

3.1 FUEL GENERATION.

A description of the rates and pathways of thermal degradation reactions which occur in the solid state during burning are the subject of this section. The basic thermal degradation mechanism leading to volatile fuel generation in polymers has been described [52, 54] as a generalized chemical bond scission process consisting of primary and secondary decomposition events as illustrated schematically in figure 6. The primary decomposition step can be main-, end-, or side-chain scission of the polymer. Subsequent thermal degradation reactions depend largely on the chemical structure of the polymer [55, 56] but typically proceed by hydrogen transfer to α - or β -carbons, nitrogen or oxygen, intramolecular exchange (cyclization), side-chain reactions, small-molecule (SO_2 , CO_2 , S_2) elimination, molecular rearrangement, and/or unzipping to monomer. Unzipping or depolymerization of vinyl polymers is characterized by a kinetic chain length or "zip length" which is the average number of monomer units produced by a decomposing radical before the radical is deactivated by termination or transfer [51]. Mathematically, the zip length is the ratio of the rate constants for initiation to termination. Aromatic backbone polymers such as polycarbonate, polyimide, and polyphenyleneoxide tend to decompose in varying degrees to a carbonaceous char residue through a complex set of reactions involving crosslinking and bond scission. A generally applicable, detailed mechanism for thermal degradation of aromatic polymers is unlikely.

The present approach avoids the need for a detailed degradation mechanism by generalizing thermal decomposition as a transient mass balance between the polymer, a reactive intermediate, and the

degradation products—fuel gases and char. Thus, we are interested in the products of thermal degradation only in terms of their contribution to the heat released during gas phase combustion. The first stage of thermal degradation produces, in a generic sense, primary volatiles (gas and tar) and possibly a primary char residue. If a primary char forms, further decomposition occurs by dehydrogenation to form the secondary gas (principally hydrogen) and a thermally stable secondary carbonaceous char.

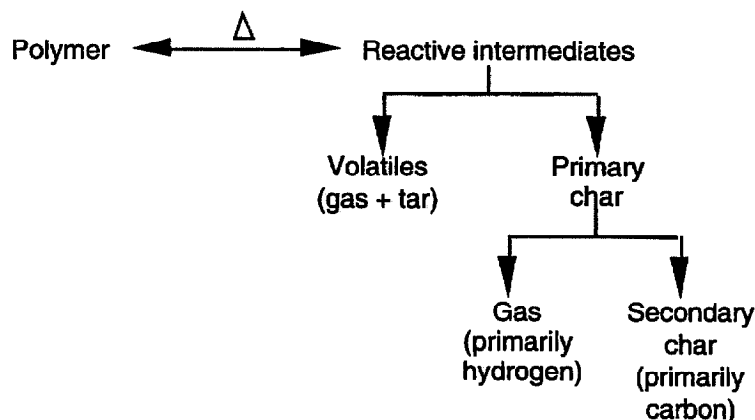


FIGURE 6. GENERALIZED THERMAL DEGRADATION MECHANISM OF POLYMERS

Figure 7 clearly shows the two-stage process of thermal decomposition for the commercial polybenzimidazole 2,2'-(m-phenylene)-5,5'-bibenzimidazole (CELAZOLE PBI, Hoechst Celanese). Plotted in figure 7 is the mass loss rate versus temperature curve of polybenzimidazole at a linear heating rate of 10 K/min in an inert (nitrogen) environment. The mass loss rate peaks corresponding to the primary and secondary charring reactions are evident.

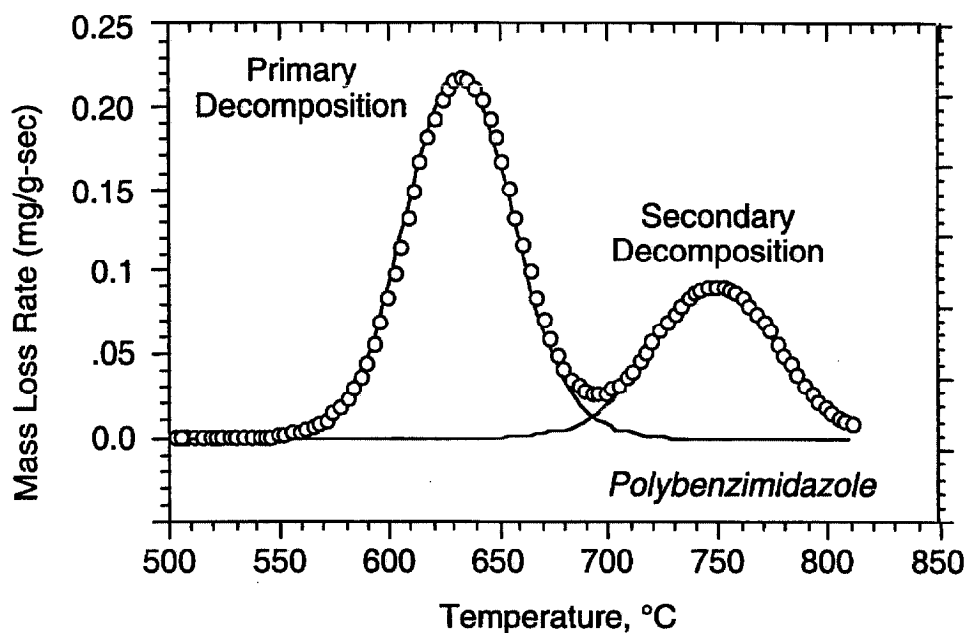


FIGURE 7. THERMOGRAVIMETRIC SCAN OF POLYBENZIMIDAZOLE AT A LINEAR HEATING RATE OF 10 K/min UNDER NITROGEN

Decomposition schemes which account for some or all of these pyrolysis products (gas, tar, primary char, secondary char, secondary gas) have been proposed wherein the decomposition steps occur sequentially (series), simultaneously (parallel), or in some combination of series/parallel steps [37, 57, 58, 59, 60, 61, 62, 63, 64, 65, 66, 67]. Three of these mechanistic pyrolytic reaction schemes for cellulose have been reviewed recently [66] including the single-step first-order model [65], an uncoupled three-step parallel model [60], and a coupled three-step series-parallel model [58, 67]. The single-step and three-step uncoupled models have a fixed char yield as an adjustable parameter while the three-step coupled model has a variable char yield. All of the models predict rate-dependent peak decomposition temperatures. Variable (n-th)- order decomposition kinetics have been fit to mass loss data for char-forming polymers with reasonable success using reaction order [68] and empirical weighting factors [69] as adjustable parameters. However, little insight is gained into the reaction pathways from these curve-fitting exercises.

A simple, solid-state fuel generation model has been derived [70] from the following assumptions about the process of polymer thermal degradation in fires:

1. A reactive intermediate I^* is generated in the polymer dissociation (initiation) step which is in rapid dynamic equilibrium with the parent polymer, P , but is consumed in the process of gas and char formation such that its concentration never becomes appreciable and decreases slowly over time as the polymer is consumed. Consequently, the rate of change of reactive intermediate with time is insignificant compared to the rate of polymer consumption, gas production, and char formation so that for computational purposes the change in intermediate concentration with time is neglected. This is the stationary-state hypothesis.
2. Thermal decomposition of primary char to secondary char and gas is slow compared to the formation of the primary char at typical flaming surface temperatures of 400-700°C. Consequently, only the primary char is considered in formulating the reaction set for the mass loss model.
3. The thermal degradation environment in the pyrolysis zone of a burning solid polymer is non-oxidizing or anaerobic. Dissolved molecular oxygen and oxygen diffusion into the pyrolysis zone of the solid are considered negligible with respect to their effects on gas and char formation so that solid-state oxidation reactions can be neglected in the fuel generation model for polymers in fires. This assumption does not preclude the possibility of surface mass loss due to thermoxidative reactions at the polymer-air interface under nonflaming conditions, e.g., thermogravimetric (TGA) experiments conducted in air or smoldering combustion.

Figure 8 shows data [71] for a variety of pure, unfilled polymers plotted as the char yield measured after flaming combustion in a fire calorimeter versus the char residue at $900 \pm 100^\circ\text{C}$ for the same material after anaerobic pyrolysis. It is seen that the char yield of a material in a fire is essentially equal to its residual mass fraction after pyrolysis in an oxygen-free environment at temperatures representative of the char temperature in a fire. Although oxidative degradation products have been identified at the surface of noncharring olefinic polymers after flaming combustion [56, 72], the data in figure 8 suggest that oxidation reactions are insignificant in the pyrolysis zone of a burning polymer as evidenced by the close agreement between fire char yield and anaerobic pyrolysis residue.

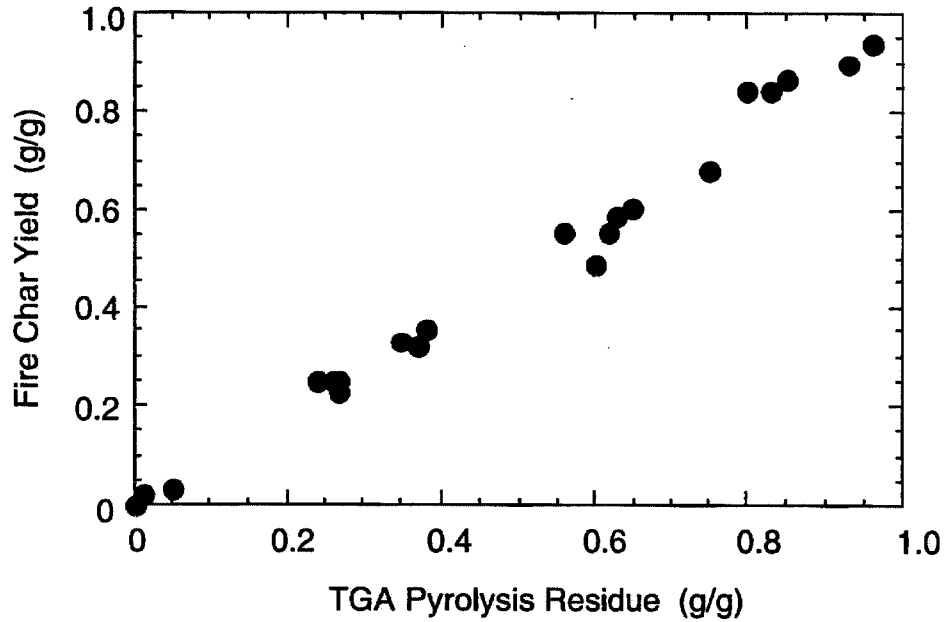


FIGURE 8. FIRE CHAR YIELD VERSUS ANAEROBIC PYROLYSIS RESIDUE FOR A VARIETY OF POLYMERS

The generalized combustion and pyrolysis schemes of figures 1 and 6, respectively, in combination with assumptions 1-3 lead to the simplified kinetic model for polymer burning which is shown in figure 9.

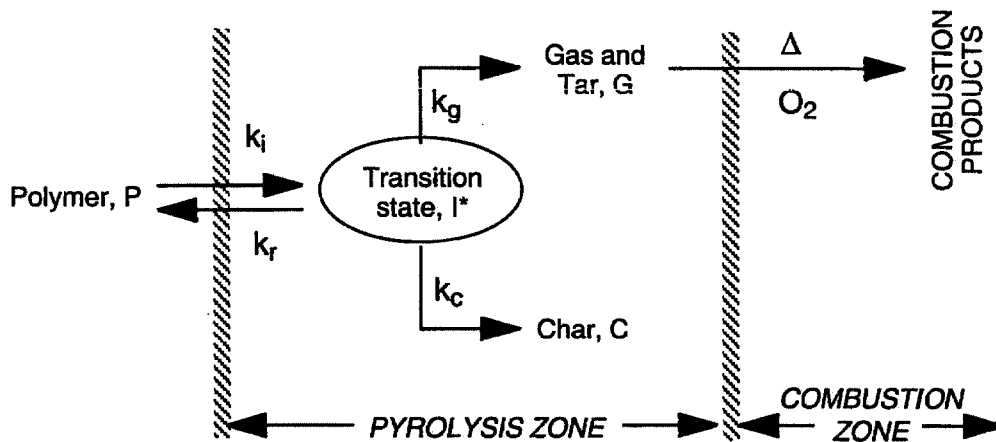
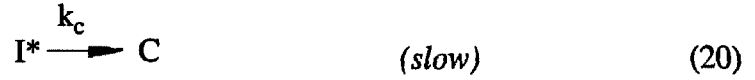
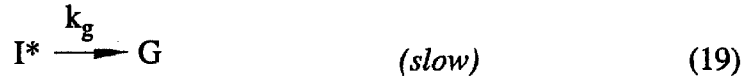
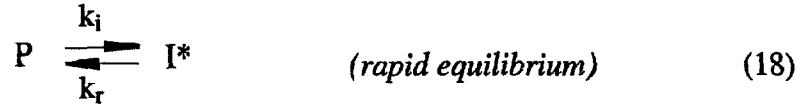


FIGURE 9. THERMAL DEGRADATION MODEL FOR POLYMERS IN FIRES

This simplified scheme reduces thermal degradation of polymer P to a single step involving parallel reactions of an active intermediate I^* to form to gas G and char C. In figure 9, k_i is the rate constant for initiation, and k_r , k_g , and k_c are the rate constants for termination by recombination (k_r), hydrogen transfer to gaseous species (k_g), and crosslinking to char (k_c), respectively. The rate constants are assumed to have an Arrhenius temperature dependence of the form $k(T) = A \exp[-E/RT]$ where A and E are the frequency factor and activation energy, respectively, at temperature T. Neglecting solid-state oxidation the thermal decomposition reactions are



and the system of rate equations for the species at time, t , is

$$\frac{dP}{dt} = -k_i P + k_r I^* \quad (21)$$

$$\frac{dI^*}{dt} = k_i P - (k_r + k_g + k_c) I^* \quad (22)$$

$$\frac{dG}{dt} = k_g I^* \quad (23)$$

$$\frac{dC}{dt} = k_c I^* \quad (24)$$

According to the stationary-state hypothesis, $dI^*/dt \approx 0$ so that equation 22 provides the useful result

$$I^* = \left[\frac{k_i}{k_r + k_g + k_c} \right] P = K P$$

where $K = k_i / (k_r + k_g + k_c)$ is the pseudo-equilibrium constant for the polymer dissociation reaction. As the ratio of initiation to termination rate constants, K represents the kinetic chain length for degradation by depolymerization [51, 73]. Substituting $I^* = K P$ into equations 21, 23, and 24,

$$\frac{dP}{dt} = -[k_i - K k_r] P \quad (25)$$

$$\frac{dG}{dt} = k_g K P \quad (26)$$

$$\frac{dC}{dt} = k_c K P \quad (27)$$

With $I^* \ll P, G, C$, the total mass balance in terms of the initial mass, m_0 , is

$$m_0 = P + G + C + I^* \approx P + G + C \quad (28)$$

From equations 25-28 with $dm_o/dt = 0$

$$\frac{dP}{dt} = -\frac{dC}{dt} - \frac{dG}{dt} = -[k_i - Kk_r]P \quad (29)$$

The sensible mass of the sample as measured, for example, in a TGA experiment or fire calorimeter test is

$$m = P + C + I^* \approx P + C$$

and with equation 26

$$\frac{dm}{dt} = \frac{dP}{dt} + \frac{dC}{dt} = -\frac{dG}{dt} = -Kk_g P \quad (30)$$

Equation 29 can be solved immediately for P in the isothermal case with initial condition $P = P_o = m_o$ @ $t = 0$,

$$P = m_o \exp\left(-[k_i - Kk_r]t\right) \quad (31)$$

Substituting the isothermal result for P into equation 30 and separating variables

$$\int_{m_o}^m dm' = -\int_0^t Kk_g m_o \exp(-k_p t) dt \quad (32)$$

where k_p in the exponential of the integrand on the right-hand side of equation 32 is the overall rate constant for pyrolysis and is assumed to have the Arrhenius form

$$k_p = k_i - Kk_r = K(k_g + k_c) = A \exp\left(-\frac{E_a}{RT}\right) \quad (33)$$

in terms of the global activation energy E_a and frequency factor A for pyrolysis. The isothermal solution of equation 32 is

$$\frac{m(t)}{m_o} = 1 - \left[\frac{k_g}{k_g + k_c}\right] \left(1 - e^{-k_p t}\right) \quad (34a)$$

or

$$\frac{m(t)}{m_o} = Y_c(T) + \left[1 - Y_c(T)\right] e^{-k_p t} \quad (34b)$$

Equation 34 shows that as $t \rightarrow \infty$ the residual mass approaches an equilibrium value at constant temperature given by

$$Y_c(T) = \frac{m(\infty)}{m_o} = \frac{k_c}{k_g + k_c} \quad (35)$$

where $Y_c(T)$ is the equilibrium residual mass fraction or char yield at temperature T in terms of the rate constants for gas and char formation. Equation 35 predicts a finite char yield at infinite time if $k_c > 0$ and zero char if $k_c = 0$.

The physical significance of a temperature-dependent, equilibrium char yield as the ratio of rate constants for gas and char formation is consistent with the use of group contributions for the char forming tendency of polymers developed by Van Krevelen [52, 53] (see the following section). If k_g and k_c have Arrhenius forms, equation 35 can be written

$$Y_c(T) = \left[1 + \frac{A_g}{A_c} \exp \left[-(E_g - E_c)/RT \right] \right]^{-1} \quad (36)$$

where E_c , E_g and A_c , A_g are the activation energies and frequency factors for char and gas formation, respectively. The crossover temperature, T_{cr} , is defined [66] as the temperature at which the rates of gasification and crosslinking are equal, i.e., when $k_g = k_c$,

$$T_{cr} = \frac{(E_g - E_c)}{R \ln[A_g/A_c]} \quad (37)$$

It follows from equation 35 that the crossover condition, $k_g = k_c$, corresponds to the equilibrium residual mass fraction, $Y_c(T_{cr}) = 0.50$.

If $Y_c(T)$ is the char yield at a temperature above the major mass loss transition or is independent of temperature then $Y_c(T) = \mu = \text{constant}$ and equation 34 is the solution for the isothermal mass loss history of a filled polymer with a nonvolatile mass fraction μ satisfying the rate law

$$\frac{dm}{dt} = -k_p (m - \mu m_o) \quad (38)$$

although equation 38 was not assumed *a priori* in the present derivation.

The previous results were derived for the isothermal (constant temperature) case but many processes of interest are conducted under nonisothermal conditions, e.g., thermogravimetric analyses at constant heating rate or fuel generation in the pyrolysis zone of a burning polymer. To calculate the instantaneous mass fraction $m(t)/m_o$ during a constant heating rate experiment where $dT/dt = \text{constant} = \beta$, begin by eliminating P between equations 29 and 31 and integrating

$$\int_{m_o}^m dm' = (1 - Y_c) \int_{P_o}^P dP' \quad (39)$$

or since $P_o = m_o$,

$$\frac{m(T)}{m_o} = Y_c(T) + [1 - Y_c(T)] \frac{P(T)}{P_o} \quad (40)$$

For nonisothermal conditions $P(T)/P_o$ in equation 40 is obtained from equation 29 as

$$\int_{P_0}^P \frac{dP'}{P'} = - \int_0^t k_p dt' = - \frac{A}{\beta} \int_{T_0}^T \exp\left(-\frac{E_a}{RT}\right) dT' \quad (41)$$

where the constant heating rate $\beta = dT/dt$ transforms the variable of integration from time t to temperature T ; and A , E_a are the global frequency factor and activation energy of pyrolysis, respectively.

The right-hand side of equation 41 is the exponential integral which has no closed form solution. An approximate solution for the exponential integral which is accurate to within 2% over the range of activation energies and temperatures encountered in thermal analysis and combustion is [74]

$$- \frac{A}{\beta} \int_{T_0}^T \exp\left(-\frac{E_a}{RT}\right) dT' \approx \frac{-ART^2}{\beta(E_a + 2RT)} \exp\left(-\frac{E_a}{RT}\right) = \frac{-k_p RT^2}{\beta(E_a + 2RT)} \quad (42)$$

Defining

$$y = \frac{k_p RT^2}{\beta(E_a + 2RT)} \quad (43)$$

the solution of equation 41 takes the form

$$\frac{P(T)}{P_0} = e^{-y} \quad (44)$$

Substituting equation 44 into equation 40, the residual mass fraction in a constant heating rate experiment is

$$\frac{m(T)}{m_0} = Y_c(T) + [1 - Y_c(T)] e^{-y} \quad (45)$$

which is the same form as the isothermal solution (equation 34). Recent work [75] on the thermal degradation of polymers in fires shows that pseudo first-order mass loss kinetics (e.g., equation 45) are a good approximation to n -th order kinetics at constant heating rate for typical reaction orders $n \leq 4$.

Figure 10 shows the agreement of equation 45 with nonisothermal experimental data for phenolic triazine, a char-forming thermoset polymer with $E_a = 178$ kJ/mol and $A = 10^9$ sec⁻¹ determined from isothermal weight loss experiments. Solid lines in figure 10 are the fits of equation 45 to experimental data (open symbols) at linear heating rates $\beta = 1, 5,$ and 20 K/min. The dashed line is the temperature dependent residual mass $Y_c(T)$ calculated from equation 36 for an energy barrier to char formation $E_g - E_c = +30$ kJ/mol and frequency factor ratio $A_g/A_c = 17$ determined in separate isothermal experiments [70]. The agreement of this simple model with experimental data is seen to be very good for this polymer up to temperatures $\approx 700^\circ\text{C}$ where secondary char formation, which was neglected in the model, begins.

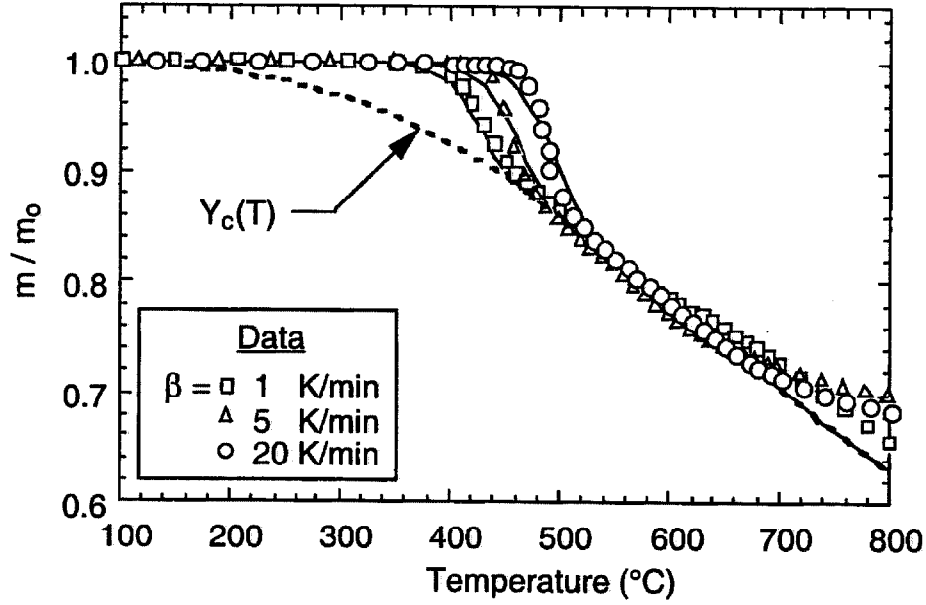


FIGURE 10. COMPARISON OF THERMAL DEGRADATION MODEL TO NONISOTHERMAL TGA DATA (NITROGEN PURGE) FOR A PHENOLIC TRIAZINE THERMOSET POLYMER

The fractional mass loss rate during a linear temperature ramp is obtained by differentiating equation 45 with respect to time,

$$\begin{aligned} \frac{-1}{m_0} \frac{dm(T)}{dt} &= (1 - Y_c(T)) \frac{de^{-y}}{dt} + (1 - e^{-y}) \frac{dY_c(T)}{dt} \\ &= (1 - Y_c(T)) k_p(T) e^{-y} + \beta Y_c(T) (1 - Y_c(T)) \frac{E_a - E_c}{RT^2} (1 - e^{-y}) \end{aligned} \quad (46)$$

Since the rate of change of $Y_c(T)$ is small compared to the fractional mass loss rate at pyrolysis (see figure 10), the approximation $Y_c(T) = \mu = \text{constant}$ is made so that $dY_c/dt = 0$ and equation 46 simplifies to

$$\frac{-1}{m_0} \frac{dm(T)}{dt} = (1 - \mu) k_p e^{-y} \quad (47)$$

The peak value of the fractional mass loss rate can be found by differentiating equation 47 with respect to time and setting this second derivative of the residual mass fraction equal to zero,

$$-\frac{d^2}{dt^2} \left(\frac{m(T)}{m_0} \right) = \beta(1 - \mu) \frac{d}{dT} [k_p e^{-y}] = (1 - \mu) k_p e^{-y} \left(\frac{\beta E_a}{RT^2} - k_p \right) = 0 \quad (48)$$

Equation 48 has two roots: the trivial case $\mu = 1$ and

$$k_p(\text{max}) = \frac{\beta E_a}{RT_p^2} \quad (49)$$

where T_p is the temperature at maximum mass loss rate during the course of the linear heating history. For example, $T_p = 635^\circ\text{C}$ at the peak fractional mass loss rate of 0.23 mg/g-s for the primary decomposition of polybenzimidazole at a constant heating rate of 10 K/min in figure 7.

An analytic result for the peak fractional mass loss rate in a constant heating rate experiment is obtained by substituting equation 49 into equation 47

$$\left. \frac{-1}{m_o} \frac{dm}{dt} \right|_{\max} = (1 - \mu) \frac{\beta E_a}{e^r RT_p^2} \quad (50)$$

where the exponent r of the natural number e in the denominator has the value

$$r = \left[1 + \frac{2RT_p}{E_a} \right]^{-1} \quad (51)$$

For the usual case where $E_a \gg 2RT_p$, equation 50 simplifies to

$$\left. \frac{-1}{m_o} \frac{dm}{dt} \right|_{\max} \approx (1 - \mu) \frac{\beta E_a}{eRT_p^2} \quad (52)$$

Once A and E_a have been determined, the heating rate dependent temperature at peak mass loss rate T_p is obtained from the root E_a/RT_p of equation 49 written in the form

$$\ln \left[\frac{E_a}{RT_p} \right]^2 + \left[\frac{E_a}{RT_p} \right] + \ln \left[\frac{\beta R}{AE_a} \right] = 0 \quad (53)$$

The effect of heating rate on peak mass loss temperature T_p embodied in equation 53 is not insignificant when comparing laboratory ($\beta \approx 10$ K/min) and fire ($\beta \approx 300$ K/min) heating rates. To illustrate this effect, pyrolysis experiments were conducted under a nitrogen atmosphere in a commercial thermogravimetric analyzer at various linear heating rates [70]. Figure 11 shows the experimental data for the temperature at peak mass loss rate T_p for samples weighing ≤ 5 milligrams. Polymers tested include a linear semicrystalline thermoplastic polyethylene (PE), $E_a = 264$ kJ/mol, $\mu = 0$ [76, 77], which degrades to short hydrocarbon chains by random chain scission; a linear amorphous thermoplastic polymer poly(methylmethacrylate) (PMMA), $E_a = 160$ kJ/mol, $\mu = 0$ [76, 77], which thermally degrades to monomer by an unzipping mechanism; and a highly crosslinked, amorphous, thermoset polymer phenolic triazine (PT), $E_a = 178$ kJ/mol, $\mu = 0.7$ [70, 74], which degrades by decyclization, crosslinking, and charring.

The accuracy of equation 52 was tested by measuring the peak mass loss rate at the decomposition temperatures plotted in figure 11 for PMMA, PE, and PT. The measured peak mass loss rates are compared in figure 12 to the peak mass loss rates calculated using equation 52 with the previous activation energies and pyrolysis residues for these polymers along with the peak mass loss temperatures plotted in figure 11. Close proximity of the data to the equivalence line on the log-log plot indicates good agreement between measured and calculated peak mass loss rate using equation 52 at heating rates ranging from $\beta = 1$ to 200 K/min.

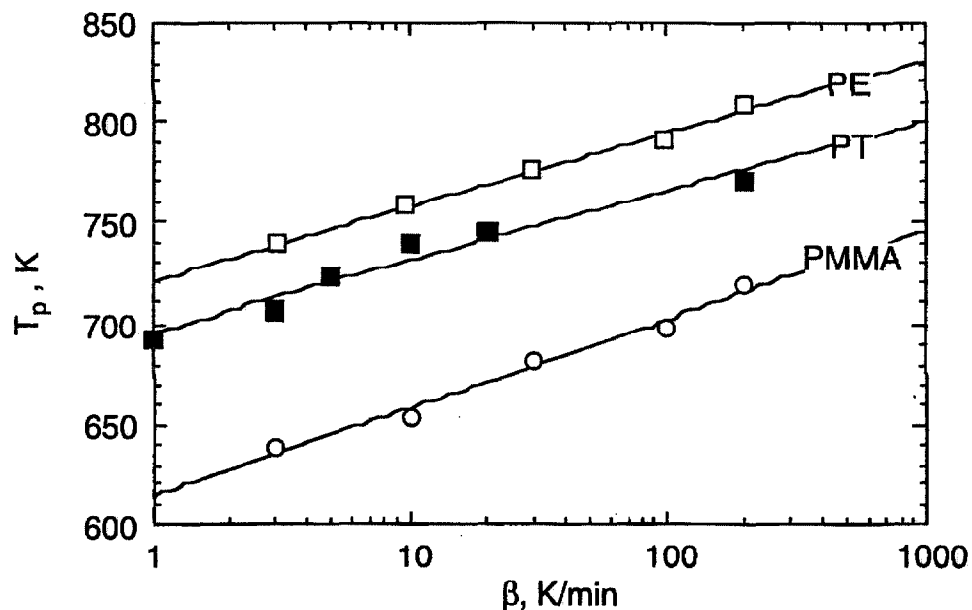


FIGURE 11. PEAK MASS LOSS TEMPERATURE VERSUS HEATING RATE FOR POLYMETHYLMETHACRYLATE (PMMA), POLYETHYLENE (PE), AND PHENOLIC TRIAZINE (PT)

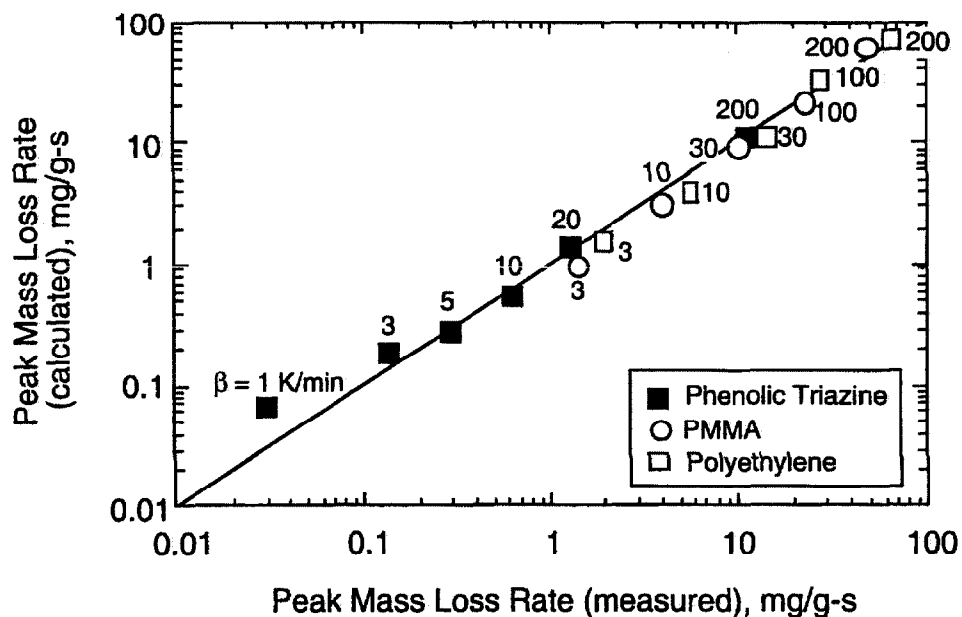


FIGURE 12. CALCULATED VERSUS MEASURED PEAK MASS LOSS RATE IN TGA FOR PMMA, POLYETHYLENE, AND PHENOLIC TRIAZINE AT INDICATED HEATING RATES, $\beta = 1, 3, 5, 10, 20, 30, 100,$ and 200 K/min

3.2 DECOMPOSITION TEMPERATURE.

Intrinsic fire resistance requires short-term thermal stability at fire temperatures as discussed in previous sections. Van Krevelen [52, 73] identified a number of experimental indices which can be used to characterize the short-term thermal stability of a polymer. The indices which are determined from temperature scanning thermogravimetry experiments at linear heating rates $\beta \approx 3-10$ K/min

are $T_{d,0}$, the temperature in Kelvin at which the polymer weight loss is just measurable; $T_{d,1/2}$, the temperature at which the weight loss reaches 50% of its final value; $T_{d,max}$, the temperature at the maximum rate of weight loss; and E_a , the activation energy for pyrolysis. Noting that all of these temperatures depend on heating rate and that $T_{d,max}$ is identical to T_p in the present work, Van Krevelen proposed the following interrelationships based on tabulated data for 37 polymers (all temperatures are Kelvin):

$$T_{d,0} = 0.9 T_{d,1/2} \quad (54)$$

$$T_{d,max} \equiv T_p \approx T_{d,1/2} \quad (55)$$

$$T_{d,1/2} \approx 423 + E_a \text{ (kJ/mol)} \quad (56)$$

Equations 54-56 imply that T_p or $T_{d,1/2}$ can be used as the primary indicator of thermal stability with the other indices being roughly estimated from it. A plot of T_p versus E_a from thermogravimetric analyses of various polymers [52, 73] at heating rates on the order of $\beta = 3$ K/min is shown in figure 13. The trend line is in qualitative agreement with equation 56, but the correlation coefficient is too low (< 0.5) for predictive purposes.

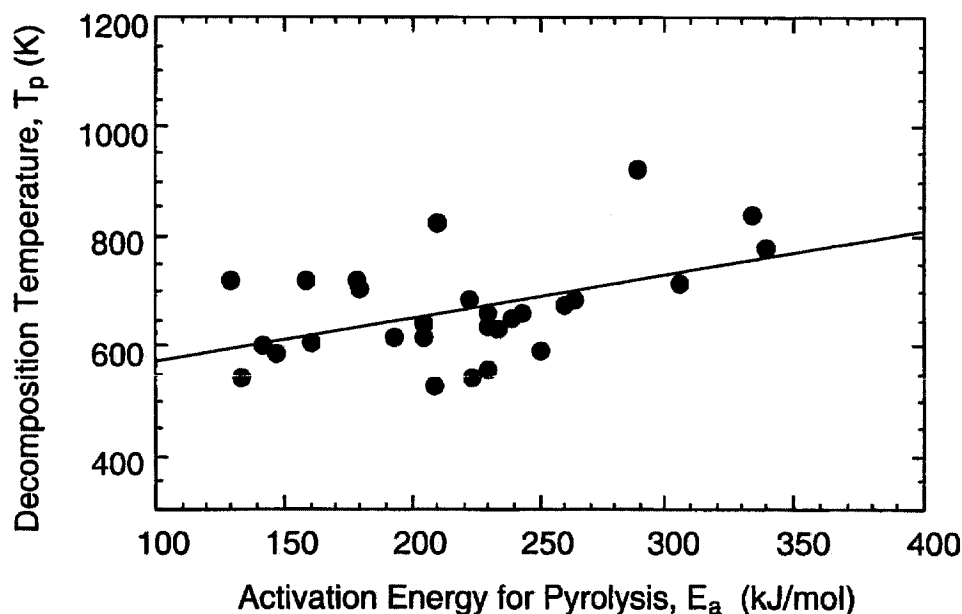


FIGURE 13. DEPENDENCE OF DECOMPOSITION TEMPERATURE ON ACTIVATION ENERGY FOR PYROLYSIS

Despite the general trend of T_p increasing with E_a in figure 13, the scatter is relatively high because of the variation in the frequency factor A between materials and its influence on E_a/T_p embodied in equation 53. In the following paragraphs we derive the proportionality between T_p and E_a from Arrhenius kinetics (i.e., equation 53) and show that it is material specific.

The Arrhenius relation for the temperature dependence of reaction rate constants, e.g., $k_p = A \exp[-E_a/RT]$, was originally derived with the assumption that the reactants are at equilibrium with a high-energy intermediate state and could proceed to products with no further energy requirements [78, 79]. Dynamic equilibrium between the dissociating polymer P and activated complex I^* (equation 18) satisfies this condition and implies a thermodynamic significance for the pyrolysis

kinetic parameters A and E_a . From the definition of the free energy at equilibrium and equation 33,

$$\ln K = \ln \left[\frac{k_p}{k_g + k_c} \right] = -\frac{\Delta G^*}{RT} = -\left[\frac{\Delta H^*}{RT} - \frac{\Delta S^*}{R} \right] \quad (57)$$

where as previously, k_p is the global rate constant for pyrolysis and k_g and k_c are the rate constants for gas and char formation, respectively. In equation 57, ΔG^* , ΔH^* , and ΔS^* are the molar free energy, enthalpy, and entropy of pyrolysis, respectively. Assuming Arrhenius forms for k_p , k_g , and k_c , it follows that

$$k_p = A e^{-E_a/RT} = \left[(k_g + k_c) e^{\Delta S^*/R} \right] e^{-\Delta H^*/RT} \quad (58)$$

where $A = (k_g + k_c) e^{\Delta S^*/R} = (k_p/K) e^{\Delta S^*/R}$ is the pre-exponential factor, and $E_a = \Delta H^*$ is the global activation enthalpy for anaerobic mass loss (pyrolysis). From equation 58 with $k_p = \beta E_a / RT_p^2$ (equation 49) at peak mass loss rate, the entropy change for the solid \rightarrow gas phase transition at temperature T_p is

$$\Delta S^*(\beta) = R \ln \left(\frac{K A R T_p^2 / E_a}{\beta} \right) \quad (59)$$

If $\Delta G^* = 0$ for this [dynamic] equilibrium process then $K = 1$ and a molecular heating rate can be defined having units (K/s)

$$\beta^* \equiv \frac{A R T_p^2}{E_a}$$

The molecular heating rate β^* is a constant if changes in A, E_a , or their ratio A/E_a compensate [80] for changes in T_p^2 with β (see figure 11). Rewriting equation 53 as

$$\frac{E_a}{R T_p} = \ln \left[\frac{A R T_p^2}{\beta E_a} \right]$$

and substituting $\beta^* = A R T_p^2 / E_a$ into the logarithmic term, the peak pyrolysis rate temperature can be expressed as

$$T_p(\beta) = \frac{E_a}{R \ln[\beta^*/\beta]} \quad (60a)$$

Figure 14 shows the data of figure 11 plotted as T_p versus $1/\ln(\beta^*/\beta)$ according to equation 60a with β^* adjusted to obtain slope E_a/R for PE ($E_a = 264$ kJ/mol), PT ($E_a = 178$ kJ/mol), and PMMA ($E_a = 160$ kJ/mol). It is seen that, to within the expected accuracy of E_a/R ($\pm 10\%$), the intercept in figure 14 which is unconstrained in the fitting exercise to obtain β^* passes through the origin as required by equation 60a. The correlation coefficient for all of the plots in figure 14 is better than 99% over the relatively narrow range of heating rates $\beta = 1-200$ K/min fitted for the extrapolation. From the β^* in figure 14 and typical $R T_p^2 / E_a \approx 20$ K, the frequency factors for pyrolysis are $A \approx \beta^*/20$ K = $10^{17} - 10^{12}$ s⁻¹, typical of frequency factors encountered in studies of polymer pyrolysis [81, 82].

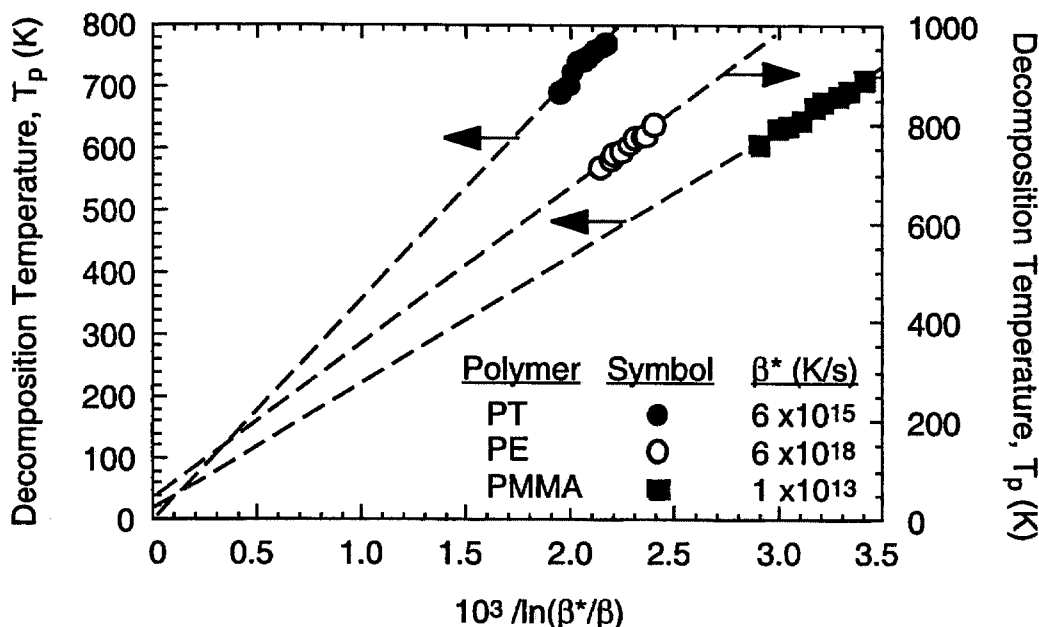


FIGURE 14. PEAK PYROLYSIS TEMPERATURE VERSUS RECIPROCAL OF THE NATURAL LOGARITHM OF THE REDUCED HEATING RATE ACCORDING TO EQUATION 60 (Dashed lines have slope E_a/R for indicated β^* .)

Substituting $\beta^* = ART_p^2/E_a$ into equation 59 gives $\Delta S(\beta) = R \ln[\beta^*/\beta]$, which has the same form as the statistical thermodynamic entropy if β^*/β is the equilibrium number of states having energy E_a at temperature T_p . The analogy between β^*/β and N can be shown by defining temperatures in the vicinity of the peak pyrolysis temperature $T_1 = (T_p - \Delta T/2)$ and $T_2 = (T_p + \Delta T/2)$ with ΔT the width of the pyrolysis peak such that $\Delta T \ll T_p$. It is found (c.f., method of section 5) that for a first-order decomposition process at constant heating rate the characteristic width of the mass loss transition (pyrolysis peak) in degrees Kelvin is $\Delta T \approx RT_p^2/E_a$. Thus $\beta^* = ART_p^2/E_a \approx A\Delta T$. The time interval corresponding to this temperature range is $\Delta t = \Delta T/\beta$ so that $\beta^*/\beta \approx (A\Delta T)/(\Delta T/\Delta t) = A\Delta t \equiv N$ where N is the number of molecular collisions occurring in time Δt at temperatures in the vicinity of T_p with sufficient energy E_a to spontaneously produce gas and/or char.

Thus, $\Delta S(\beta) = R \ln[\beta^*/\beta] = R \ln[N]$ is consistent with the statistical thermodynamic interpretation of entropy as the logarithm of the number of excited states at T_p and equation 60a can be written in the various forms

$$T_p(\beta) = \frac{E_a}{R \ln[\beta^*/\beta]} = \frac{\Delta H^*}{R \ln[N]} = \frac{\Delta H^*}{\Delta S^*(\beta)} \quad (60b)$$

The inverse proportionality between decomposition temperature T_p and $\ln[N]$ is physically realistic because the greater the number of collisions resulting in mass loss (low heating rate = large Δt = large $\ln[N]$) the earlier the peak mass loss temperature will occur in the heating program (low T_p) since the fractional mass loss for complete pyrolysis is independent of heating rate (see section 4.1).

Although equation 60a is easily recast in the form of equation 56 by defining a reference temperature $T_o = 423$ K corresponding to a reference heating rate $\beta = \beta_o$, it is not sufficiently

accurate for predictive purposes. For this reason, Van Krevelen extended the use of additive molar group contributions which he had previously used to calculate the equilibrium glass transition and melting temperatures to the calculation of the thermal decomposition temperature [52, 91]. Additive molar group contributions had long been used for quantitative prediction of the equilibrium properties of ordinary molecules and polymers, e.g., heats of combustion [83], thermophysical and transport properties [84, 85], chemical reactivity [86], and biological activity [87]. In Van Krevelen's method of calculating the thermal decomposition temperature, the molar thermal decomposition function $Y_{d,1/2}$ is related to the product of the polymer repeat unit molecular weight M and the decomposition temperature viz.

$$M \cdot T_{d, 1/2} = Y_{d, 1/2} \quad (61)$$

From the previous discussion it is apparent that $T_{d,1/2} = T_p$ is a kinetic (rate-dependent) parameter and so the molar thermal decomposition function must be also. Comparison of equations 60b and 61 show that for a particular heating rate β_0 the molar decomposition function is related to the molar heat ΔH^* and entropy $\Delta S^*(\beta_0)$ of decomposition as

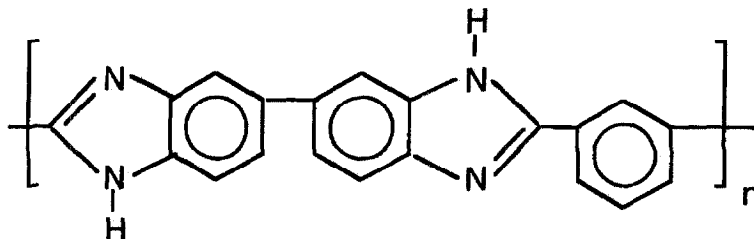
$$Y_{d, 1/2} = Y_{d, 1/2}(\beta_0) = \frac{M \cdot \Delta H^*}{\Delta S^*(\beta_0)}$$

The decomposition temperature is calculated by summing the individual molar decomposition functions $Y_{d, 1/2}^i$ for each chemical group of the molar mass M_i comprising the repeat unit

$$T_{d, 1/2} = \frac{Y_{d, 1/2}}{M} = \frac{\sum_{i=1}^N n_i Y_{d, 1/2}^i}{\sum_{i=1}^N n_i M_i} \quad (62)$$

Equation 62 is the same form as those used to predict the glass transition and melting temperatures of polymers using the appropriate values for the molar group contributions [52]. The empirical method of Van Krevelen for calculating thermal decomposition temperature requires a molar group contribution $Y_{d, 1/2}^i$ for each of the chemical groups comprising the polymer. These molar group contributions were determined for decomposition temperatures measured at a linear heating rate $\beta_0 \approx 3$ K/min. The following example is illustrative of the additive method of group contributions developed by Van Krevelen.

To calculate the decomposition temperature of the fire-resistant commercial polymer CELAZOLE PBI (2,2'-(m-phenylene)-5,5'-bibenzimidazole), first write the chemical repeat unit structure for PBI

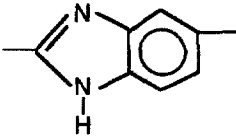


Comparing the chemical structure to tabulated group contributions for $Y_{d, 1/2}^i$, the data in table 1 can be assembled. From table 1 and equation 62 the peak decomposition temperature of PBI at low heating rate is

$$T_p = \frac{(2)(105) + (1)(65)}{(2)(116.12) + 76.09} \cdot 1000 = 892 \text{ K}$$

which is in general agreement with the literature value [52] $T_p \approx 903 \text{ K}$ and the primary decomposition peak in figure 7.

TABLE 1. GROUP CONTRIBUTIONS TO THE DECOMPOSITION TEMPERATURE OF POLYBENZIMIDAZOLE AFTER VAN KREVELEN [91]

Group	Quantity	M_i (g/mol)	$\frac{Y_{d, 1/2}^i}{(K \cdot \text{kg/mol})}$
	2	116.12	105
	1	76.09	65

While calculation of T_p for commercial PBI is straightforward, it is often the case that the molar group contributions are not available in the literature for predicting decomposition temperatures of new, thermally stable polymers containing novel backbone and pendant structures. Recognizing this limitation of the group contribution method, Bicerano [84] generalized the additive scheme using graph theory to develop atomic connectivity indices which replace the larger chemical groups in the traditional additive approach as the principle descriptors of the topology of the polymer repeat unit. Bicerano's approach is still empirical in that the connectivity indices must be determined from experimental data or by correlation with known group contributions. However, once the connectivity indices are determined for a particular property, that property may be predicted for any chemical structure for which the atomic (as opposed to group) indices are known. The connectivity index method of predicting polymer properties from atomic composition can be accomplished with a hand calculator but is more typically implemented using a stand-alone computer code (SYNTHIA) or accessed as a module in molecular modeling software (Molecular Simulations, Inc., San Diego, CA).

Molecular dynamics simulations of polymer thermal degradation have also recently become available [88]. Molecular dynamics simulations are the most fundamental and powerful approach to understanding and predicting polymer thermal stability because, unlike the additive approaches, molecular dynamics can predict the thermal decomposition products of polymers [89].

Table 2 is a listing of the temperature at peak mass loss rate T_p [90, 91] and the pyrolysis residue μ [90, 91, 92] at $850 \pm 50^\circ\text{C}$, for the indicated polymers heated in an inert environment at a linear heating rate $\beta = 3\text{-}10 \text{ K/min}$ according to standard methods [93]. Also listed are the limiting oxygen index [56, 90, 94] and the Underwriters Laboratory UL 94 Vertical or Horizontal burn ranking [95]. The limiting oxygen index [96] is the minimum concentration (volume percent) of oxygen in the environment required to sustain candlelike burning (downward flame spread) after ignition of a 3- x 6- x 150-mm specimen at room temperature using a small methane flame. A limiting oxygen index above 20 would indicate self-extinguishing behavior when ignited at ambient (20°C , 20 volume percent oxygen) conditions.

TABLE 2. PEAK PYROLYSIS TEMPERATURE (T_p), PYROLYSIS RESIDUE (μ), LIMITING OXYGEN INDEX (LOI), AND UL 94 RANKING OF SOME POLYMERS (Values in parentheses are calculated estimates.)

Polymer	T_p ($^{\circ}\text{C}$)	μ (%)	LOI (%)	UL 94 Ranking
Polybenzobisoxazole (PBO)	789	75	56	V-0
Polyparaphenylene	652	75	55	(V-0)
Polybenzimidazole (PBI)	630	70	42	V-0
Polyamideimide (PAI)	628	55	45	V-0
Polyaramide (KEVLAR)	628	43	28	V-0
Polyetherketoneketone (PEKK)	619	62	40	V-0
Polyetherketone (PEK)	614	56	40	V-0
Polytetrafluoroethylene (PTFE)	612	0	95	V-0
Polyetheretherketone (PEEK)	606	50	35	V-0
Polyphenylsulfone (PPSF)	606	44	38	V-0
Polypara(benzoyl)phenylene (PX)	602	66	41	V-0
Fluorinated Cyanate Ester	583	44	(40)	V-0
Polyphenylenesulfide (PPS)	578	45	44	V-0
Polyetherimide (PEI)	575	52	47	V-0
Polypyromellitimide (PI)	567	70	37	V-0
Liquid Crystal Polyester	564	38	40	V-0
Polycarbonate (PC)	546	25	26	V-2
Polysulfone (PSF)	537	30	30	V-1
Polyethylene (PE)	505	0	18	HB
Polyamide 6 (PA6)	497	1	21	HB
Polyethylenenaphthalate (PEN)	495	24	32	V-2
Polyphthalamide	488	3	(22)	HB
Phenolic Triazine Cyanate Ester (PT)	480	62	30	V-0
Polyethyleneterephthalate (PET)	474	13	21	HB
Cyanate ester of Bisphenol-A (BCE)	470	33	24	V-1
Polydimethylsiloxane (PDMS)	444	0	30	HB
Acrylonitrile-butadiene-styrene (ABS)	444	0	18	HB
Polyurethane elastomer (PU)	422	3	17	HB
Polymethylmethacrylate (PMMA)	398	2	17	HB
Polychlorotrifluoroethylene	380	0	95	V-0
Polystyrene (PS)	364	0	18	HB
Polyoxymethylene (POM)	361	0	15	HB
Poly(α -methylstyrene)	341	0	18	HB
Polyvinylchloride (PVC)	270	11	50	V-0

The UL 94 test [97] ranks materials with respect to their time to self-extinguish after a 10-second Bunsen burner ignition. A V-0 rating in this table means that a thin (< 1-mm-thick) specimen of the polymer self-extinguished in a vertical orientation within 10 seconds after removal of the flame while V-1 and V-2 rankings indicate self-extinguishing behavior in less than 30 seconds, without and with flaming droplets, respectively. A rating of HB means that the specimen burns in a horizontal orientation at a rate which is less than that specified for a particular sample thickness. The LOI and UL flammability test results are indicative of the propensity for flame spread on a thin polymer sample in the absence of an external heat flux, but they are poor predictors of full-scale fire performance in a radiant environment [16].

The data in table 2 are ranked in descending order of peak decomposition temperature (short-term thermal stability). High thermal stability results from strong primary and secondary bonds and low hydrogen content all of which favor recombination/crosslinking (charring) reactions during thermal degradation rather than the hydrogen transfer/termination reactions which lead to mass loss [98]. Excluding the halogenated polymers, it is seen that high thermal stability roughly correlates with flame resistance.

In concluding this section we note that the thermal decomposition temperature is a *kinetic* parameter which is heating rate dependent (c.f., equations 53 and 60), unlike the glass transition and melting temperatures which are equilibrium (thermodynamic) properties. Thus, the decomposition temperature calculated from molar group contributions obtained empirically from arbitrarily slow heating rates under-predicts the polymer burning surface temperature in a fire where heating rates may be orders of magnitude higher (c.f., figure 11 and equation 17).

4. THERMODYNAMICS.

This section addresses the intensive, equilibrium (rate independent) quantities relevant to fire behavior which are dependent on, and calculable from, the polymer chemical composition and structure. Included in this category are the char yield, heat of gasification, and chemical heat of combustion.

4.1 CHAR YIELD.

Char is the carbonaceous solid which remains after flaming combustion of the polymer. The char yield is the mass fraction of char based on the original weight of material. Charring reduces the volatile fuel content in a fire and is thought to act as a heat and mass transfer barrier which lowers the chemical heat release rate in bench-scale flaming combustion tests (e.g., cone/fire calorimeters). Figure 6 demonstrates that the char yield in a fire is equal to the anaerobic pyrolysis residue at the flaming surface temperature. Thus, char formation takes place in an oxygen-free environment where solid-state oxidation reactions are slow compared to polymer dissociation and gas/char formation. The equivalence between the char yield and pyrolysis residue of a material permits a molecular interpretation of this important material fire parameter using the large volume of published thermogravimetric data and its correlation with chemical structure.

Equation 47 shows that the kinetic fuel generation rate of a polymer during transient heating decreases linearly with increasing pyrolysis residue or char yield. This trend of decreasing flammability with increasing pyrolysis residue has long been known for small flame tests [99] and the limiting oxygen index [92, 100] and for this reason much work has been focused on empirical correlations between charring and polymer structure [91, 92]. Figure 15 shows the data in table 2 plotted to illustrate the well-known relationship between limiting oxygen index (LOI) and char yield (μ) for polymers. Halogenated polymers are clearly outliers from the correlation line plotted in figure 15, confirming a gas phase component to the LOI measurement.

Figure 15 shows that char yield alone is not a good predictor of the oxygen concentration at flame extinguishment (LOI). Moreover, the extinguishment condition is a function of both char yield and gas phase chemistry as indicated by the pronounced effect of halogens on LOI. Since the flame temperature of diffusion flames increases with the oxygen concentration, the flame heat flux also increases. In fact, the flame heat flux of burning polypropylene increases in proportion to the oxygen fraction of the environment [101]. Thus, a critical oxygen concentration at extinguishment (LOI) means that a critical flame heat flux is required to sustain steady burning of the specimen. Since the UL 94 flammability test is conducted at a fixed (ambient) oxygen fraction, the flame heat flux is not an adjustable parameter so material properties alone will determine whether the material will sustain flaming combustion after removal of the ignition source.

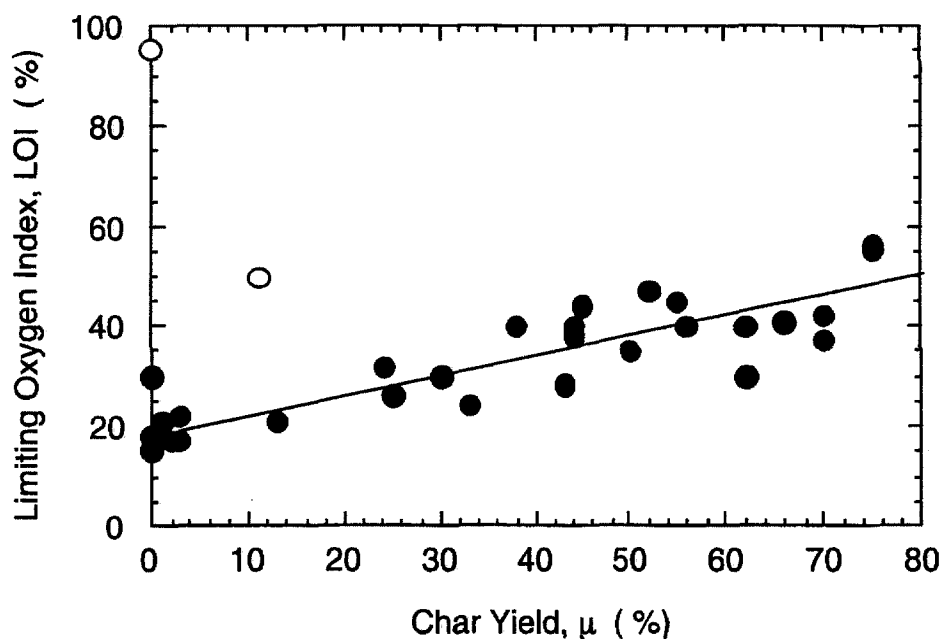


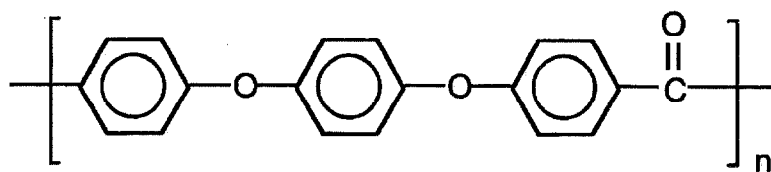
FIGURE 15. RELATIONSHIP BETWEEN LIMITING OXYGEN INDEX AND CHAR YIELD FOR HALOGEN (○) AND NONHALOGEN (●) POLYMERS FROM TABLE 2

Pyrolysis/char residue has the character of a thermodynamic quantity since it depends only on temperature and the composition of the material through the enthalpy barriers to gas and char formation, E_g , E_c in equation 36. More precisely, char yield is a statistical thermodynamic concept wherein the total free energy of the char system at a particular (reference) temperature is the sum of the individual group contributions [91,92]. Figure 16 shows the equilibrium residual mass fraction *versus* temperature for activation energy barriers $\Delta E_{g-c} = 10, 20, 30,$ and 40 kJ/mol according to equation 36 for $A_g/A_c = 20$.

Van Krevelen [91, 92] has devised a method for calculating the pyrolysis residue (\approx char yield) of a polymer from its chemical composition and the observation that the char forming tendency of different groups is additive and roughly proportional to the aromatic (i.e., nonhydrogen) character of the group. Analogous to equation 62 for computing T_p from group contributions, the char yield is calculated by summing the char forming tendency per mole of carbon of the chemical groups, $C_{FT,i}$ and dividing by the molecular weight of the repeat unit

$$Y_c = \frac{C_{FT}}{M} \times M_{\text{carbon}} \times 100 = \frac{\sum_{i=1}^N n_i C_{FT,i}}{\sum_{i=1}^N n_i M_i} \times 1200 \quad (63)$$

The $C_{FT,i}$ are the amount of char per structural unit measured at 850°C divided by 12 (the atomic weight of carbon), i.e., the statistical amount of carbon equivalents in the char per structural unit of polymer. Negative corrections are made for aliphatic groups containing hydrogen atoms in proximity to char-forming groups because of the possibility for disproportionation and subsequent volatilization of chain-terminated fragments which are no longer capable of crosslinking. The method is empirical and relatively simple to use as illustrated in the following example to predict the char yield of the fire resistant, semicrystalline thermoplastic poly(etheretherketone) (PEEK) having the chemical structure



The group contributions to char formation for the chemical groups in PEEK are listed in table 3.

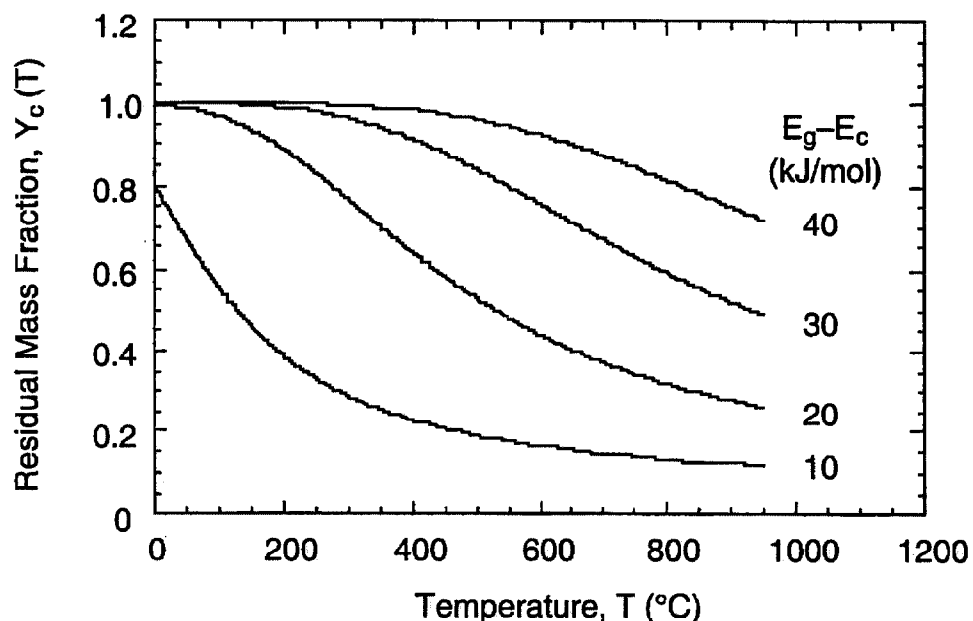


FIGURE 16. EQUILIBRIUM MASS FRACTION VERSUS TEMPERATURE FOR ENERGY BARRIERS TO GASIFICATION ($\Delta E_{g-c} = 10, 20, 30,$ and 40 kJ/mol according to equation 36.)

TABLE 3. GROUP CONTRIBUTIONS TO THE CHAR RESIDUE OF POLY(ETHERETHERKETONE) FROM REFERENCE 91

Group	Quantity	M_i (g/mol)	$C_{FT,i}$ (C-equivalents)
	3	76.10	4
	2	16.00	0
	1	28.01	0

The char yield calculated with equation 63 for poly(etheretherketone)

$$Y_c(850^\circ\text{C}) = \frac{(3 \cdot 4) + (2 \cdot 0) + 0}{(3 \cdot 76.10 \text{ g/mol}) + (2 \cdot 16.00 \text{ g/mol}) + 28.01 \text{ g/mol}} \cdot 12 \text{ g/mol} \times 100 = 50\%$$

is in good agreement with the measured pyrolysis residue (char yield) of poly(etheretherketone) in table 2 and in the literature [102, 103] at 850°C. The char yield of polymers under anaerobic conditions is thus well described using the additive molar contributions of the individual groups comprising the polymer.

4.2 HEAT OF GASIFICATION.

In section 3.2 the pyrolysis activation energy E_a was identified with the molar enthalpy of gasification ΔH^* . Since E_a is a thermodynamic state function, it is the sum of the enthalpies to bring the polymer solid from the solid state at the initial (room) temperature T_0 to the gaseous state at the decomposition temperature T_p . If the stored heat is ΔH_s , the enthalpy of fusion (melting) for semicrystalline polymers is ΔH_f , the bond dissociation enthalpy is ΔH_d , and the enthalpy of vaporization of the decomposition products is ΔH_v , then

$$E_a \equiv \Delta H^* = \Delta H_s + \Delta H_f + \Delta H_d + \Delta H_v \quad (64)$$

Table 4 illustrates the magnitude of these enthalpic terms on a mass basis for amorphous poly(methylmethacrylate), polystyrene, and semicrystalline polyethylene. Values are as reported in Joules per gram (J/g) or have been converted to a mass basis by dividing the molar heat by the molecular weight of the gaseous decomposition products M_g . The stored heat Δh_s was obtained by numerical integration of heat capacity versus temperature [104] from ambient up to the dissociation temperature. The dissociation (bond breaking) enthalpy Δh_d is assumed to be equal to the heat of polymerization but opposite in sign for these polymers which thermally degrade by random or end-chain scission [105]. The degradation product for polyethylene is assumed to be a tetramer (i.e., octane with $M_g = 112$ g/mol) for the purpose of calculating the heats of dissociation and vaporization on a mass basis for this polymer, and the degree of polyethylene crystallinity is taken to be 90 percent. All other enthalpies in table 4 were obtained from handbooks [104, 106] using individual monomer molecular weights M to convert the energies to a mass basis. Three values of h_g are listed for each polymer in table 4 for comparison. The uppermost values were calculated by summing the enthalpies listed in the table for each polymer. The second row of values of h_g are calculated as E_a/M_g from handbook values for E_a [104] and the M_g 's listed in the table. The h_g values in the last row of table 4 are the slope of mass loss rate versus external heat flux measurements made in fire calorimeters [46] according to equation 15.

TABLE 4. ENTHALPIES OF GASIFICATION FOR PMMA, PS, AND PE

Polymer	PMMA	PS	PE
M (g/mol)	100	104	28
M_g (g/mol)	100	104	112
	Value, J/g		
Δh_s	740	813	803
Δh_f	amorphous	amorphous	243
Δh_d	550	644	910
Δh_v	375	387	345
$h_g = \Sigma \Delta h_i$	1665	1850	2301
$h_g = E_a/M_g$	1550 ± 300	1930	2230 ± 630
h_g (measured)	1600	1800	2300

The agreement between the enthalpies of gasification calculated from the component enthalpies $\Sigma\Delta h_i$ for the solid→gas phase change, the reported activation energy for pyrolysis [107] E_a/M_g , and the reported heat of gasification h_g for the three polymers in table 4 is better than $\pm 10\%$ when the molar basis for the activation energy is the molecular weight of the degradation products. If M_g is the average molecular weight of the decomposition products, then [44]

$$h_g = \frac{\Delta H^*}{M_g} = \frac{E_a}{M_g} \quad (65)$$

and the molecular weights of the decomposition products and the starting monomer should be in the ratio

$$\frac{M_g}{M} = \frac{E_a}{M h_g} \quad (66)$$

Polymers which pyrolyze to monomer by end-chain scission (depolymerize/unzip) at near-quantitative yield such as polymethylmethacrylate, polyoxymethylene, and polystyrene should have M_g equal to the monomer molecular weight, M , i.e., $M_g/M \approx 1$. Polymers such as polyethylene and polypropylene which decompose by random scission to multimonomer fragments should have $M_g/M > 1$. In contrast, polymers with high molecular weight repeat units ($M \geq 200$ g/mol) such as nylon, cellulose, or polycarbonate which degrade by random scission, cyclization, small-molecule splitting, or chain stripping of pendant groups (e.g., polyvinylchloride) will yield primarily low molecular weight species (water, carbon dioxide, alkanes, HCl) relative to the starting monomer and should have $M_g/M < 1$. Table 5 shows the molecular weight ratio M_g/M calculated as E_a/Mh_g according to equation 66 for some of the commercial polymers listed in table 2. Global pyrolysis activation energies for the thermally stable engineering plastics listed in the last four rows of table 5 are estimated to be in the range $E_a = 275 \pm 25$ kJ/mol. Qualitative agreement is observed between the modes of pyrolysis (end-chain scission, random scission, chain stripping) and the calculated fragment molecular weight using equation 66, suggesting that the global pyrolysis activation energy determined from mass loss rate experiments is the molar enthalpy of pyrolysis of the degradation products. The heat of gasification per unit mass of original solid $h_g = (1-\mu)L_g$ increases from about 2.5 to 3.5 kJ/g as a result of the increase in stored heat at the higher decomposition temperature of thermally stable polymers such as PC, PEI, PPS, PEEK, and PAI.

In practice, the heat of gasification per unit mass of solid h_g is rarely calculated because detailed and reliable thermodynamic data for the polymer and its decomposition products are generally unavailable except for the most common polymers. Laboratory thermogravimetric analyses to determine h_g from the pyrolysis activation energy E_a require a separate determination of the average molecular weight of the gaseous thermal decomposition products (equation 65). The data in table 5 suggest that $M_g \approx 75$ -200 g/mol for most polymers which is in agreement with direct measurements $M_g = 125 \pm 50$ g/mol for the major pyrolysis products of aromatic polyimides using gas chromatography-mass spectrometry [108]. Direct laboratory measurement of h_g using differential thermal analysis (DTA) [93] and differential scanning calorimetry (DSC) [46] have been reported, but h_g is usually measured indirectly as a component of L_g in a constant heat flux gasification device or fire calorimeter [46].

4.3 HEAT OF COMBUSTION.

As stated previously polymers do not burn—their decomposition products do. Thus, it is the net heat of complete combustion of the *fuel gases*, h_c° , in equation 16 which must be known or calculable. It was shown that polymers thermally decompose to volatile fuel species and, possibly, a solid charred residue if the molecular density of aromatic/hydrogen-deficient groups is sufficient to

TABLE 5. HEATS OF GASIFICATION, PYROLYSIS ACTIVATION ENERGY, CHAR YIELD, AND CALCULATED MOLECULAR WEIGHT OF DECOMPOSITION PRODUCTS FOR SOME POLYMERS LISTED IN TABLE 2

Polymer	M (g/mol)	L _g (kJ/g)	μ (g/g)	h _g (kJ/g)	E _a (kJ/mol)	E _a /Mh _g (M _g /M)	Pyrolysis Products
PP	42	2.5	0	2.5	243	2.3	C ₂ -C ₉₀ saturated and unsaturated hydrocarbons
PE	28	2.4	0	2.4	264	3.9	
PS	104	2.2	0	2.2	230	1.0	40-60% monomer
PMMA	100	1.6	0	1.6	160	1.0	100% monomer
POM	30	2.7	0	2.7	84	1.0	100% monomer
PA 66	226	2.6	0	2.6	160	0.3	H ₂ O, CO ₂ , C ₅ HC's
PVC	62	2.5	0.1	2.8	110	0.7	HCl, benzene, toluene
Cellulose	162	3.2	0.2	2.6	200	0.5	H ₂ O, CO ₂ , CO
PT	131	5.0	0.6	2.0	178	0.3	Complex mixture of low molecular weight products
PC	254	5.3	0.3	3.7	200	<1	
PEI	592	7.7	0.5	3.9	≈ 275	<1	
PPS	108	6.6	0.5	3.3	≈ 275	<1	
PEEK	288	5.6	0.5	2.8	≈ 275	<1	
PAI	356	8.0	0.6	3.2	≈ 275	<1	
PX	180	6.4	0.7	2.2	≈ 275	<1	

allow inter- or intra-molecular crosslinking and cyclization. The net heat of complete combustion of the polymer $h_{c,p}^{\circ}$ is related to the net heats of complete combustion of the volatiles h_c° and char $h_{c,\mu}^{\circ}$ as

$$h_c^{\circ} = \frac{h_{c,p}^{\circ} - \mu h_{c,\mu}^{\circ}}{(1 - \mu)} \quad (67)$$

Thus the char fraction μ and its heat of combustion $h_{c,\mu}^{\circ}$ must be known for charring materials to calculate the heat of combustion of the fuel gases from the heat of combustion of the polymer. Elemental analysis of the charred fire residue from burned engineering polymers [109] gives an approximate carbon/hydrogen molar ratio of 5/2 so that the char repeat unit is C₅H₂ and thermochemistry calculations (see following section) give $h_{c,\mu}^{\circ} = 37$ kJ/g which compares with the average polymer heat of combustion in table 6, $h_{c,p}^{\circ} = 29 \pm 6$ kJ/g. For a char yield of 50% ($\mu = 0.5$) equation 67 predicts

$$h_c^{\circ} \approx \frac{3}{4} h_{c,p}^{\circ} \quad (68)$$

showing that the heat of combustion of the fuel gases for a charring polymer in a fire can be significantly less than the heat of combustion of the polymer itself.

At constant pressure and when no nonmechanical work is done, the heat (Q, q) and enthalpy (H, h) of a process are equal. The flaming combustion of polymers at atmospheric pressure satisfies these conditions. The high-pressure adiabatic combustion of a polymer in a bomb calorimeter satisfies these conditions approximately, since the fractional pressure change is small. Consequently, the

TABLE 6. MEASURED AND CALCULATED GROSS HEATS (Q_c) OF POLYMER COMBUSTION (Use equation 72 to convert to net heat of combustion, $h_{c,p}^{\circ}$. All values are kJ/g.)

Polymer	Measured	From Oxygen Consumption	From Heats of Formation
Polyoxymethylene	17.39	15.44	18.20
Polytetrafluoroethylene	6.68	8.38	7.57
Polyvinylalcohol	23.31	25.81	26.20
Polyethylene	47.74	48.05	46.00
Polydimethylsiloxane	19.53	18.78	N/A
Polypropylene	45.80	48.05	46.00
Polymethylmethacrylate	26.81	26.91	27.50
Poly(1,4-phenylenesulfide)	29.01	27.98	30.80
Poly(2,6-dimethyl-1,4 phenyleneoxide)	34.21	34.65	34.70
Polystyrene	43.65	42.00	41.30
Polyethyleneterephthalate	24.13	22.75	24.10
Epoxy novolac	31.37	36.58	32.06
Poly(1,4-phenyleneethersulfone)	25.42	23.34	25.70
Poly(1,4-butanediol terephthalate)	27.91	25.97	26.90
Poly(hexamethyleneadipamide)	30.90	32.74	32.80
Poly(etherketone)	31.07	30.84	31.45
Poly(benzoyl-1,4-phenylene)	38.35	34.74	35.90
Poly(p-phenylene benzobisoxazole)	29.18	26.54	29.00
Poly(m-phenyleneisophthalamide)	26.45	28.22	29.30
Aramid-arylester copolymer	25.27	28.22	29.30
Poly(p-phenyleneterephthalamide)	26.92	28.22	29.30
Poly(amideimide)	24.97	25.28	26.75
Poly(acrylonitrile-butadiene-styrene)	39.84	40.01	39.43
Bisphenol E Cyanate Ester	29.38	29.58	29.62
Polycarbonate of bisphenol-A	31.30	30.92	31.20
Hexafluorobisphenol A Cyanate Ester	18.71	20.00	19.79
Bisphenol A Cyanate Ester	29.92	30.51	30.45
Bisphenol-A Epoxy	32.50	31.10	33.50
Poly(etheretherketone)	31.28	30.75	31.50
Tetramethylbisphenol F Cyanate Ester	31.23	32.12	31.72
Poly(etherketoneketone)	31.15	30.92	31.50
Polybenzimidazole	22.22	32.16	33.40
Polyimide	26.03	24.72	26.30
Phenol Novolac Cyanate Ester	29.63	28.84	28.83
Bisphenol M Cyanate Ester	34.39	34.15	33.81
Polysulfone	30.46	30.02	31.20
Poly(bisphenol-A/aniline) benzoxazine	34.89	35.45	35.80
Polyetherimide	29.33	29.21	30.00
Polyester of hydroxybenzoic/ naphthoic acids	26.54	26.22	26.81

terms heat and enthalpy are used interchangeably in the following section on methods for determining the heat of combustion of polymers. Table 6 lists experimental values for the gross heat of combustion measured by oxygen bomb calorimetry [110] according to standard methods [111]. The second and third columns in table 6 list the gross heats of combustion calculated from

oxygen consumption thermochemistry and from molar group additivity of the heats of formation, respectively, according to the methods described in the following sections. Analysis of the data in table 6 shows that thermochemical calculations based on oxygen consumption thermochemistry or additive heats of formation are within about 5% of measured values for the gross heat of combustion of polymers.

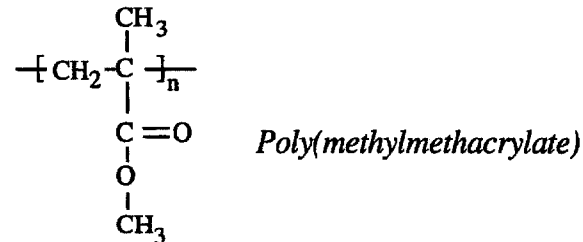
4.3.1 Calculation From Oxygen Consumption.

Heats of combustion of organic macro-molecules can be calculated from the oxygen consumed in the combustion reaction [112]. Oxygen consumption is, in fact, the basis for most modern bench- and full-scale measurements of heat release in fires [113, 114]. The principle of oxygen consumption derives from the observation that for a wide range of organic compounds, including polymers, the heat of complete combustion per mole of diatomic oxygen consumed is a constant, E , which is independent of the composition of the polymer. Mathematically,

$$E = h_{c,p}^{\circ} \left[\frac{n M}{n_{O_2} M_{O_2}} \right] = \frac{h_{c,p}^{\circ}}{r_o} = 13.1 \pm 0.7 \text{ kJ/g-O}_2 \quad (69)$$

where $h_{c,p}^{\circ}$ is the net heat of complete combustion of the polymer solid with all products in their gaseous state, n and M are the number of moles and molecular weight of the molecule or polymer repeat unit, respectively, n_{O_2} is the number of moles of O_2 consumed in the balanced thermochemical equation, and $M_{O_2} = 32 \text{ g/mol}$ is the molecular weight of diatomic oxygen. In equation 69 the quantity $r_o = [n_{O_2} M_{O_2} / nM]$ is the stoichiometric oxygen-to-fuel mass ratio.

To illustrate the thermochemical calculation of the net heat of combustion we use as an example poly(methylmethacrylate) (PMMA) which has the chemical structure



The methylmethacrylate repeat unit shown in brackets has the atomic composition $C_5H_8O_2$ so the balanced chemical equation for complete combustion is



From equation 70 it is seen that 6 moles of O_2 are required to completely convert one mole of PMMA repeat unit to carbon dioxide and water. Inverting equation 69

$$h_{c,p}^{\circ} = E \left[\frac{n_{O_2} M_{O_2}}{n M} \right] = \frac{(13.1 \text{ kJ/g-O}_2)(6 \text{ mol O}_2)(32 \text{ g O}_2/\text{mol O}_2)}{(1 \text{ mol PMMA})(100 \text{ g/mol PMMA})} = 25.15 \text{ kJ/g} \quad (71)$$

To compare the net heat of combustion to the gross heat of combustion Q_c determined by oxygen bomb calorimetry, the latent heat of vaporization of the water produced in the combustion

reaction must be added. An approximation based on the weight fraction of hydrogen in the molecule w_H is [115]

$$Q_c = h_{c,p}^{\circ} + (21.96 \text{ kJ/g}) w_H \quad (72)$$

For PMMA, $w_H = (8 \text{ g hydrogen})/(100 \text{ g monomer}) = 0.08$ so from equation 72, $Q_c = 25.15 + (21.96)(0.08) = 26.91 \text{ kJ/g}$. This is in good agreement with literature values $Q_c = 26.20 \text{ kJ/g}$ [116] and 26.64 kJ/g [115] for PMMA.

4.3.2 Calculation From Heats of Formation.

Calculation of the heat of the combustion reaction of polymers can be carried out using the principle of molar additivity of the heats of formation of the combustion products and reactants [83, 117] analogous to the previous calculations of decomposition temperature and char yield from molar quantities. The concept derives from the fact that enthalpy is a state function and therefore its change in any process is independent of the path from reactants to products. Thus, the overall enthalpy of a reaction is simply the sum of the enthalpies of the component reactions. In practice, the heat of combustion of the reaction can be calculated by subtracting the heat of formation of the products from the heat of formation of the reactants

$$\Delta H_{c,p}^{\circ} = \sum_{i=1}^n n_{p,i} H_{p,i}^{\circ} - \sum_{i=1}^n n_{r,i} H_{r,i}^{\circ} \quad (73)$$

where p and r denote products and reactants, respectively, in the standard state at 298 K.

For polymeric reactants the molar heat of formation can be estimated from the tabulated molar contributions of the chemical groups which constitute the monomer or repeat unit. Using PMMA as an example again with the monomer/repeat unit chemical structure above, the heats of formation of the methylmethacrylate constituent groups at $T = 298 \text{ K}$ are listed in table 7 after Van Krevelen [91].

TABLE 7. GROUP CONTRIBUTIONS TO THE HEAT OF FORMATION OF PMMA

Group	Qty.	$H_{r,i}$ (J/mol)	$n_{r,i} H_{r,i}^{\circ}$ (kJ/mol)
—CH ₃	2	-46,000 + 95T	- 35.38
$\begin{array}{c} \\ -C- \\ \end{array}$	1	20,000 + 140T	61.72
—CH ₂ —	1	22,000 + 102T	8.40
—O—	1	-120,000 + 70T	- 99.14
$\begin{array}{c} O \\ \\ -C- \end{array}$	1	-132,000 + 40T	- 120.08
		Total	- 184.48

Summing these group contributions gives the molar heat of formation of the methylmethacrylate monomer, $\Delta H_f = -184.48 \text{ kJ/mol}$ at standard conditions ($T = 298 \text{ K}$). The stoichiometry of complete combustion is



The tabulated standard heats of formation of the products are

$$H_p (\text{H}_2\text{O}) = -241.8 \text{ kJ/mol}; \quad H_p (\text{CO}_2) = -393.5 \text{ kJ/mol}$$

The standard heats of formation of the reactants are

$$H_r (\text{O}_2) = 0 \text{ kJ/mol}; \quad H_r (\text{PMMA}) = -184.5 \text{ kJ/mol}$$

The molar heat of combustion of PMMA is therefore

$$\begin{aligned} \Delta H_c (\text{PMMA}) &= H_{\text{prod}} - H_{\text{react}} \\ &= [5 \text{ CO}_2 + 4 \text{ H}_2\text{O}] - [\text{C}_5\text{H}_8\text{O}_2 + 6 \text{ O}_2] \\ &= [5 (-393.5 \text{ kJ/mol}) + 4 (-241.8 \text{ kJ/mol})] - [-184.5 \text{ kJ/mol} + 6 (0)] \\ &= -2748.7 \text{ kJ/mol} \end{aligned}$$

The absolute value of the gross heat of combustion per unit mass is then

$$\begin{aligned} Q_c (\text{PMMA}) &= |\Delta H_c / M| \\ &= [2748.7 \text{ kJ/mol}] / [100 \text{ g-MMA/mol}] \\ &= 27.5 \text{ kJ/g} \end{aligned}$$

which compares favorably to literature values $Q_c = 26.20 \text{ kJ/g}$ [116] and 26.64 kJ/g [115] for PMMA.

5. THERMAL-CHEMICAL COUPLING: THE PYROLYSIS ZONE.

In this section the solid-state thermochemistry of gaseous fuel generation is related to steady macroscopic burning through a characteristic dimension—the pyrolysis zone thickness. It is seen that the pyrolysis (process) zone provides the coupling between thermal diffusion and solid-state thermochemistry. According to equation 52 the peak (time-independent) kinetic heat release rate for complete combustion of volatiles generated during transient anaerobic pyrolysis at heating rate β is

$$\dot{Q}_c (\text{W/kg}) = -h_c^\circ \frac{\dot{m}_{\text{max}}}{m_o} \approx h_c^\circ \frac{\beta(1-\mu) E_a}{eRT_p^2} \quad (74)$$

From equation 16 the steady macroscopic heat release rate per unit area of burning surface, S , for a pyrolysis zone of constant thickness, δ , (see figure 4) is

$$\dot{q}_c (\text{W/m}^2) = \chi h_c^\circ \frac{\dot{m}}{S} = \chi \rho \delta h_c^\circ \frac{\dot{m}}{m_o} \quad (75)$$

where $m_o/S = \rho\delta$ is the areal density of pyrolyzing polymer. From equations 74 and 75 the ratio of the macroscopic and kinetic heat release rates at comparable surface heating rates is

$$\frac{\dot{q}_c}{\dot{Q}_c} = \chi \rho \delta \quad (76)$$

Thus, the macroscopic and kinetic heat release rates are related through the gas phase combustion efficiency χ , polymer density ρ , and pyrolysis zone thickness δ . Since χ and ρ do not vary greatly between materials, equation 76 shows that the pyrolysis zone depth provides the primary coupling between the chemical kinetics and thermal diffusion in steady burning. Thus, the concept of a distinct process zone is integral to the solid-state thermochemistry of flaming combustion.

The pyrolysis zone thickness can be estimated using the criteria that the mass loss rate falls to 1/e of the surface ($x = 0$) value at 1/e of the pyrolysis zone thickness $x = \delta/e$. Since the mass loss rate has an Arrhenius form

$$\frac{\dot{m}(\delta/e)}{\dot{m}(0)} \equiv \frac{1}{e} = \exp\left[-\frac{E_a}{R}\left(\frac{1}{T(\delta/e)} - \frac{1}{T_p}\right)\right] \quad (77)$$

Equation 77 shows that the mass loss rate falls to 1/e of the surface value for typical $E_a = 200 \pm 50$ kJ/mol when $T(\delta/e)$ is 10-20 K lower than the surface temperature T_p , i.e., $T_p - T(\delta/e) \approx 20$ K. Since $T_p - T(\delta/e) \ll T_p \approx T(\delta/e)$, equation 77 takes the simple form

$$T_p - T(\delta/e) = \frac{RT_p^2}{E_a} \quad (78)$$

Substituting equation 11 into equation 10 with $x = \delta/e$

$$T_p - T(\delta/e) = (T_p - T_o)\left(1 - \exp\left[-\frac{v}{\alpha}\frac{\delta}{e}\right]\right) \quad (79)$$

Eliminating $T_p - T(\delta/e)$ between equations 78 and 79 for $RT_p^2/(E_a(T_p - T_o)) \ll 1$,

$$\frac{v}{\alpha}\frac{\delta}{e} \approx \frac{RT_p^2}{E_a(T_p - T_o)} \quad (80)$$

or with equation 11

$$\delta = \frac{\kappa}{\dot{q}_{net}} \frac{eRT_p^2}{E_a} \quad (81)$$

For typical polymer values $T_p = 750$ K, $E_a = 200$ kJ/mol, and $\kappa(T_p) \approx 0.2$ W/m-K, equation 81 predicts $\delta \approx 0.3$ mm at a net incident heat flux, $\dot{q}_{net} = 50$ kw/m², which is in agreement with estimates $\delta \leq 1$ mm [32].

A rate-independent material flammability parameter emerges from this analysis when the kinetic heat release rate on the right side of equation 74 is normalized for heating rate

$$\eta_c(\text{J/g-K}) \equiv \frac{\dot{Q}_c}{\beta} = \frac{h_c^o(1-\mu)E_a}{eRT_p^2} \quad (82)$$

The thermokinetic flammability parameter η_c has the units and significance of a heat [release] capacity (J/g-K) when the linear heating rate is β (K/s). Substituting the heat release capacity η_c (equation 82), pyrolysis zone depth δ (equation 81), and the heating rate β (equation 17) into equation 75 recovers the thermal diffusion-limited steady heat release rate (equation 16) from the thermochemistry after cancellation of terms

$$\dot{q}_c = \chi \rho \delta \beta \eta_c = \chi \rho \left[\frac{\kappa}{\dot{q}_{net}} \frac{eRT_p^2}{E_a} \right] \left[\frac{\dot{q}_{net}^2}{\kappa \rho h_g} \right] \left[\frac{h_c^\circ (1 - \mu) E_a}{eRT_p^2} \right] = \chi \frac{h_c^\circ}{L_g} \dot{q}_{net} \quad (83)$$

Obtaining the macroscopic heat release rate from the derived diffusion (β) thermokinetic (η_c) and thermal-chemical coupling (δ) parameters shows that the thermochemistry of diffusion-limited steady burning is self-consistent.

6. CHEMICAL STRUCTURE AND FIRE BEHAVIOR.

Sections 1 through 5 demonstrate that the time to ignition and steady burning rate of a polymer in a particular fire environment (i.e., external heat flux) can be expressed in terms of material properties which are calculable from the chemical structure of the polymer and/or measurable using standard laboratory thermal analyses. In this concluding section we apply chemical structure-fire property relationships to the calculation of polymer flammability, heat flux dependence of the burning temperature, and heat release rate.

6.1 FLAMMABILITY.

The data in figure 15 and table 2 suggest that both the halogen content and the char yield μ are needed to correlate all of the polymer flammability data. If the effect of halogens on polymer flammability is primarily to alter the gas phase combustion efficiency χ [118] the concept of a critical heat release rate developed in section 2.2 can be extended to flame extinguishment in the UL 94 test.

Figure 17 is a plot of UL 94 ranking *versus* the quantity μ +LOI for all of the polymers in table 2. It is apparent from this plot that a μ +LOI value below about 55% is associated with sustained burning (UL HB) while polymers with μ +LOI greater than 55% tend to self-extinguish (UL V-0/1/2) after removal of the small flame ignition source. Polymers with values of μ +LOI > 95% do not burn or ignite even after repeated attempts at ignition (e.g., UL 94-5V) and also exhibit very low heat release rate in bench-scale fire tests [16, 17, 18]. These observations are consistent with a critical energy release rate (section 2.2) for burning in the UL 94 test.

Combining equations 9 and 16 the energy release rate in the UL 94 test can be represented as

$$\dot{q}_c = \chi (1 - \mu) \frac{h_c^\circ}{h_g} \left(\dot{q}_{external} + \dot{q}_{flame} - \dot{q}_{critical} \right)$$

Accounting for gas phase combustion inhibition with the approximation $\chi \approx (1 - LOI)$ derived from combustion efficiency data [46] and limiting oxygen indices [56] of burning polymers, the non-burning condition after removal of the Bunsen burner flame in the UL 94 test when $\dot{q}_{ext} = 0$ is

$$\begin{aligned}
\mu + \text{LOI} &= 1 - \left(\frac{h_g}{h_c^o} \right) \left(\frac{\dot{q}_{c,cr}}{\dot{q}_{\text{flame}} - \dot{q}_{\text{critical}}} \right) + (\mu \cdot \text{LOI}) \\
&= 1 - \left(\frac{3 \text{ kJ/g}}{30 \text{ kJ/g}} \right) \left(\frac{100 \text{ kW/m}^2}{35 \text{ kW/m}^2 - 15 \text{ kW/m}^2} \right) + (0.25)(0.25) \\
&\approx 0.56
\end{aligned}$$

where typical values for the heat of gasification (table 5), heat of combustion (table 6), flame heat flux [119], critical heat flux [46], and the critical energy release rate $\dot{q}_{c,cr} = 100 \text{ kW/m}^2$ (section 2.2) were assumed. The small product term $\mu \cdot \text{LOI}$ was evaluated at $\mu = \text{LOI} = 0.25$ corresponding to approximate values at the flammability transition $\mu + \text{LOI} \approx 0.5$ in figure 17. The critical energy release rate criteria for burning in the UL 94 test predicts a transition (V-1, V-2) from flammable (HB) to nonflammable (V-0) behavior for both halogen and nonhalogen polymers at $\mu + \text{LOI} \approx 0.56$. This prediction is in excellent agreement with the data in figure 17 and suggests a predominantly additive effect of solid-state and gas-phase mechanisms of flame resistance (i.e., $\mu + \text{LOI}$) with synergistic effects embodied in the product term $\mu \cdot \text{LOI}$.

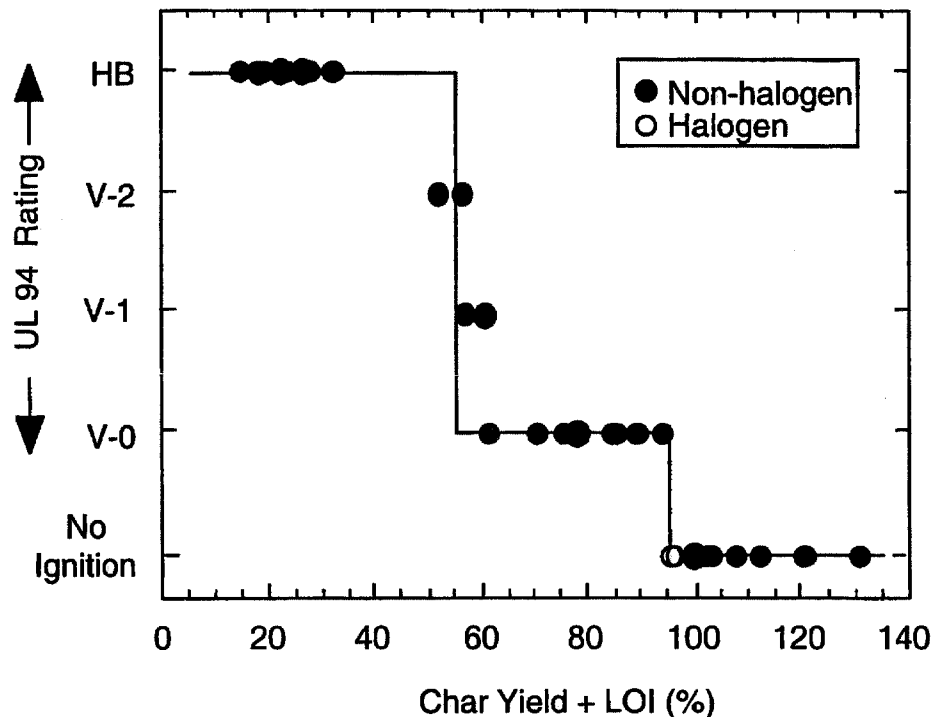


FIGURE 17. UNDERWRITERS LABORATORY UL 94 RANKING OF FLAMMABILITY VERSUS THE COMBINED PARAMETER $\mu + \text{LOI}$ FOR THE POLYMERS IN TABLE 2 SHOWING TRANSITION FROM BURNING TO SELF-EXTINGUISHING BEHAVIOR AT $\mu + \text{LOI} \approx 0.56$ (56%)

6.2 BURNING TEMPERATURE.

In section 2 we made the ad hoc assumption that the ignition and steady-burning temperatures at constant heat flux in the fire environment were equal to the peak pyrolysis temperature calculated from group contributions or measured at constant heating rate in a laboratory environment (e.g.,

thermal analysis instrument) in order to establish a relationship between the chemical structure of polymers and their fire behavior. To test this hypothesis we calculate the surface burning temperature of PMMA as a function of external heat flux. Equation 17 gives the effective heating rate at the polymer surface which when substituted into equation 60, gives the peak pyrolysis temperature as a function of heat flux. Figure 18 shows data (private communication M.A. Delichatsios, Factory Mutual Research, 1999) for the measured surface temperature of 1-inch-thick PMMA slabs during steady nonflaming gasification (under nitrogen) at the indicated radiant external heat fluxes. For nonflaming gasification, $\dot{q}_{\text{flame}} = 0$, so from equation 17 with $\dot{q}_{\text{ext}} = \dot{q}_{\text{net}} \gg \dot{q}_{\text{cr}}$ and $\kappa\rho c = 5 \times 10^5 \text{ W}\cdot\text{s}\cdot\text{m}^{-4}\cdot\text{K}^{-2}$ we calculate the surface heating rates β shown along the top of figure 18. From the calculated β with $\beta^* = 10^{13} \text{ K/s}$ (see figure 14) and $E_a = 160 \text{ kJ/mol}$ for PMMA, equation 60 predicts the steady surface temperature versus heat flux relationship indicated by the solid line in figure 18. The measured and calculated surface temperatures for steady-state gasification are in reasonable agreement for PMMA—suggesting that thermal-diffusion limited chemical kinetics influences the fuel generation process for thermally thick samples.

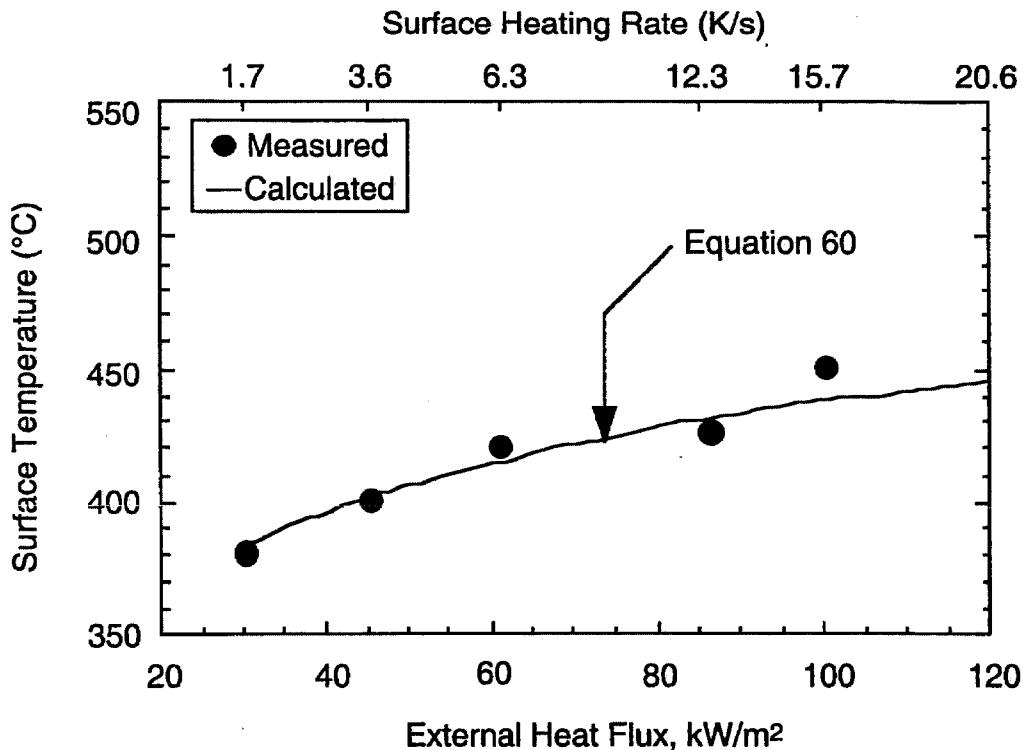


FIGURE 18. SURFACE TEMPERATURE OF PMMA VERSUS EXTERNAL RADIANT HEAT FLUX FOR STEADY NONFLAMING GASIFICATION

6.3 HEAT RELEASE RATE.

Figure 19 shows experimental data [16, 17, 18, 19, 48, 120, 121] for the 3-minute average heat release rate measured in a fire calorimeter operating on the oxygen consumption principle [122]. Incident heat flux on the thermally thick polymer samples was $\dot{q}_{\text{ext}} = 50 \text{ kW/m}^2$. The trend of decreasing heat release rate in flaming combustion with increasing char yield of the polymer is obvious in figure 19. However, the nonlinear relationship between heat release rate and char yield suggests that simple rule-of-mixtures behavior based on the reduced fuel fraction is not the underlying mechanism. As discussed in section 2 char acts as a thermal- and mass-diffusion barrier as it accumulates on the surface of burning polymers. Table 2 shows that charring polymers

also tend to be more thermally stable and their flammability depends on both solid-state (charring) and gas phase (combustion) reactions. Deviation of polyvinylchloride (PVC) from the trend line for hydrocarbon polymers in figure 19 highlights the effect of gas phase combustion inhibition by halogens on heat release rate as well as small-scale flammability tests.

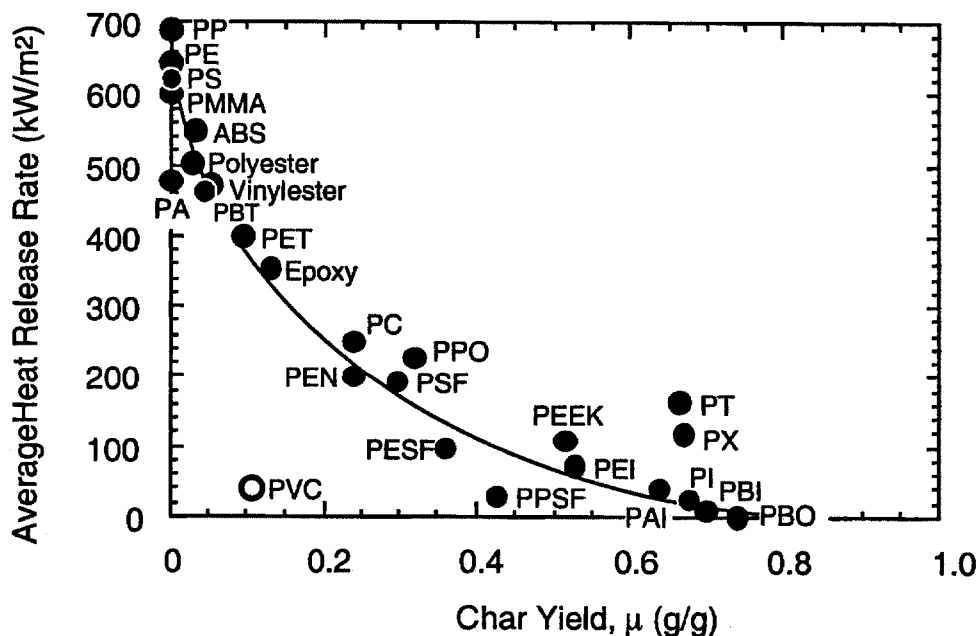


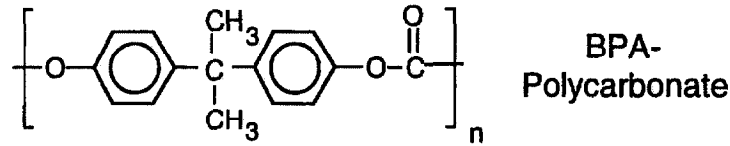
FIGURE 19. AVERAGE FLAMING HEAT RELEASE RATE VERSUS CHAR YIELD FOR POLYMERS LISTED IN TABLE 2 (Not listed in table 2 are polypropylene (PP), (Polyester)-, (Vinylester)-, and (Epoxy)-thermosets, polybutyleneterephthalate (PBT), poly(2,6, dimethyl)phenylene oxide (PPO), and polyethersulfone (PESF).)

Section 2 provided the relationship between the thermal (κ , ρ , and c) and combustion (T_{ign} , μ , h_g , and $h_{c,p}^{\circ}$) properties of materials and their steady heat release rate during flaming combustion (equation 16) derived from a mass and energy balance at the surface

$$\dot{q}_c = \chi h_c^{\circ} \dot{m}_g = \chi (1 - \mu) \frac{h_c^{\circ}}{h_g} \dot{q}_{net} = \chi \frac{h_c^{\circ}}{L_g} \dot{q}_{net}$$

Methods were presented for obtaining the solid combustion properties from molar group additivity calculations ($T_{ign} \approx T_p$, μ , and $h_{c,p}^{\circ}$) or thermochemical calculations (h_g). Methods for calculating equilibrium thermophysical properties of polymers (κ , ρ , c) and their temperature dependence from molar group additivity calculations are well established [83, 85], as are the measurement techniques for these properties [93, 123] and were not reviewed in the chapter. Thus, in principle all of the fundamental thermal and combustion properties necessary to predict the flaming heat release rate of burning polymers in a given fire environment (χ , \dot{q}_{net}) are calculable to a first approximation from the polymer chemical structure. As an example we calculate the steady (average) heat release rate of a char forming polymer (bisphenol-A polycarbonate) from its chemical structure using the concepts developed in this chapter and compare the result to experimental data for this polymer plotted in figure 19.

The chemical structure of bisphenol-A polycarbonate (e.g., LEXAN™) is



From the chemical groups in polycarbonate we calculate the following properties from their molar group contributions [91]:

- Density at pyrolysis temperature $\rho (T_p) \approx 1040 \text{ kg/m}^3$ reference 73
- Pyrolysis temperature $T_p = 683 \text{ K}$ equation 62
- Char yield $\mu = 0.24$ equation 64
- Net Heat of Combustion (solid) $h_{c,p}^\circ = 29.7 \text{ kJ/g}$ equations 71 and 72

Note that the calculated pyrolysis temperature of 683 K is significantly below the measured pyrolysis temperature for polycarbonate reported both in table 2 and reference 52. From these properties and the literature value $E_a = 200 \text{ kJ/mol}$ for polycarbonate [124] we calculate the following parameters:

- The *net* heat of complete combustion of the fuel gases

$$h_c^\circ = \frac{h_{c,p}^\circ - \mu h_{c,\mu}^\circ}{(1 - \mu)} = \frac{29.7 \text{ kJ/g} - (0.24) 37 \text{ kJ/g}}{(1 - 0.24)} = 27.4 \text{ kJ/g} \quad (\text{equation 67})$$

- The surface heating rate for polycarbonate having $\kappa\rho c = 7.5 \times 10^5 \text{ W}\cdot\text{s}^{-1}\cdot\text{m}^{-4}\cdot\text{K}^{-2}$ [46]

$$\beta \approx \frac{1}{2} \frac{(50 \text{ kW/m}^2)^2}{\left(7.5 \times 10^5 \frac{\text{W}\cdot\text{s}}{\text{m}^4\cdot\text{K}^2}\right)(683 \text{ K} - 300 \text{ K})} \approx 4.4 \text{ K/s} \quad (\text{equation 17b})$$

- The pyrolysis zone depth

$$\begin{aligned} \delta &= \frac{e\kappa}{q_{\text{net}}} \frac{RT_p^2}{E_a} = \frac{(2.718)(0.2 \text{ W/m}\cdot\text{K})(8.314 \text{ J/mol}\cdot\text{K})(683 \text{ K})^2}{(50 \text{ kW/m}^2)(200 \text{ kJ/mol})} && (\text{equation 81}) \\ &= 2 \times 10^{-4} \text{ m} \end{aligned}$$

- The heat release capacity

$$\begin{aligned} \eta_c (\text{J/g}\cdot\text{K}) &\equiv \frac{h_c^\circ (1 - \mu) E_a}{eRT_p^2} && (\text{equation 82, table 5}) \\ &= \frac{(27.4 \text{ kJ/g})(1 - 0.24)(200 \text{ kJ/mol})}{(2.718)(8.314 \text{ J/mol}\cdot\text{K})(683 \text{ K})^2} \\ &= 395 \text{ J/g}\cdot\text{K} \end{aligned}$$

Collecting these terms in equation 84 and approximating the gas phase combustion efficiency as

$$\chi \approx 1 - \text{LOI} = (1 - 0.26) = 0.74 \quad (\text{see section 4.1})$$

calculate the average heat release rate in flaming combustion from equation 83

$$\begin{aligned} \dot{q}_c &= \chi \rho \delta \beta \eta_c = (0.74)(1040 \text{ kg/m}^3)(2 \times 10^{-4} \text{ m})(4.4 \text{ K/s})(395 \text{ J/kg-K}) \\ &= 268 \text{ kW/m}^2 \end{aligned}$$

which agrees with the experimental value $\dot{q}_c = 250 \text{ kW/m}^2$ reported in figure 19 for bisphenol-A polycarbonate to within the accuracy of the calculation and the experimental accuracy ($\pm 15\%$) of the heat release rate measurement. Note that the much simpler calculation using equation 16 with an average enthalpy of gasification, $h_g \approx 3.0 \pm 0.8 \text{ kJ/g}$ (table 5) also gives reasonable agreement with measured values for the chemical heat release rate of burning polycarbonate.

$$\dot{q}_c = \chi \frac{h_c^\circ}{L_g} \dot{q}_{\text{net}} = (0.74) \left(\frac{27.4 \text{ kJ/g}}{(3 \text{ kJ/g}) / (1 - 0.24)} \right) (50 \text{ kW/m}^2) = 257 \text{ kW/m}^2$$

7. REFERENCES.

1. C.L. Segal, ed., High Temperature Polymers, New York, Marcel Dekker, Inc., 1967.
2. Engineered Materials Handbook, Volume 2, Engineering Plastics, Metals Park, OH, ASM International, 1988.
3. P.E. Cassidy, Thermally Stable Polymers, New York: Marcel Dekker, Inc., 1980.
4. P.M. Hergenrother, "Recent Developments in Poly(Arylene Ether)s Containing Heterocyclic Units," *J. Macromol. Sci.*, 31: 731-738, 1994.
5. P.M. Hergenrother and S.J. Havens, "Polyimides Containing Quinoxaline and Benzimidazole Units," *Macromolecules*, 27(17): 4659-4664, 1994.
6. B.J. Jensen, P.M. Hergenrother, and G. Nwokogu, "Polyimides With Pendent Ethynyl Groups," *Polymer*, 34 (3): 630-635, 1993.
7. D.J. Riley, A. Gungor, S.A. Srinivasan, M. Sankarapandian, et al., "Synthesis and Characterization of Flame-Resistant Poly(Arylene Ether)s," *Polym. Eng. and Sci.*, 37(9): 1501-1511, 1997.
8. G.W. Meyer, S.J. Pak, Y.J. Lee, and J.E. McGrath, "New High-Performance Thermosetting Polymer Matrix Material Systems," *Polymer*, 36(11): 2303-2309, 1995.
9. C.D. Smith, A. Gungor, P.A. Wood, S.C. Liptak, et al., "Hydrolytically Stable Thermoplastic and Thermosetting Poly(Arylene Phosphine Oxide) Material Systems," *Makromol. Chemie-Macromol. Symp.*, 74: 185-188, 1993.
10. F.W. Harris, F.M. Li, S.H. Lin, J.C. Chen, et al., "New Organo-Soluble Polyimides for Optical, Microelectronic, and Fiber Applications," *Macromol. Symp.*, 122: 33-38, 1997.
11. M.R. Unroe and L.S. Tan, "The Design of High Use Temperature Organic Oligomeric and Polymeric Materials for Air Force Applications," *Proceedings of the 42nd International SAMPE Symposium*, 42(2): 1071-1077, 1987.
12. P.M. Hergenrother, "Heat-Resistant Polymers," in J.I. Kroschwitz (ed.), High Performance Polymers and Composites, New York, John Wiley & Sons, 1996, pp. 366-392.
13. Fire and Smoke: Understanding the Hazards, Washington, D.C., National Academy Press, 1986.
14. M.M. Hirschler (ed.), Carbon Monoxide and Human Lethality: Fire and Non-Fire Studies, London, Elsevier Applied Science, 1993.
15. G.E. Hartzell, "Combustion Products and Their Effects on Life Safety," in A.E. Cote (ed.), Fire Protection Handbook, 18th ed., Sec. 4, Chapter 2, Quincy, MA, National Fire Protection Association, 1997.
16. A.F. Grand, "Heat Release Calorimetry Evaluations of Fire-Retardant Polymer Systems," *Proceedings of the 42nd International SAMPE Symposium* 42(2): 1062-1070, 1987.

17. W. Bassett, "Flame-Retardant Thermoplastic Materials for Aircraft Interiors," Proceedings of the Fire-Retardant Chemicals Association Meeting, San Antonio, TX, March 12, 1989, pp. 143-152.
18. J. Koo, S. Venumbaka, P. Cassidy, J. Fitch, A. Grand, and J. Burdick, "Evaluation of Thermally Resistant Polymers Using Cone Calorimetry," Proceedings of the 5th International Conference on Fire and Materials, San Antonio, TX, February 23-24, 1998, pp. 183-193.
19. M.J. Scudamore, P.J. Briggs, and F.H. Prager, "Cone Calorimetry—A Review of Tests Carried Out on Plastics for the Association of Plastics Manufacturers in Europe," *Fire and Materials*, 15: 65-84, 1991.
20. V. Babrauskas, "Specimen Heat Fluxes for Bench-Scale Heat Release Rate Testing," *Fire and Materials*, 19: 243-252, 1995.
21. C. Helado, ed., Flammability Handbook for Plastics, 4th ed., Lancaster, PA, Technomic, 1990, Chapter 4.
22. J.G. Quintiere and M.T. Harkelroad, "New Concepts for Measuring Flame Spread Properties," in T.Z. Harmathy (ed.), Fire Safety Science and Engineering; Special Technical Publication 882, Philadelphia, PA, American Society for Testing and Materials, 1985, pp. 239-267.
23. "Standard Test Method for Behavior of Materials in a Vertical Tube Furnace at 750°C," ASTM E 136, ASTM Fire Test Standards, 3rd ed., Philadelphia, PA, American Society for Testing of Materials, 1990, pp. 230-238.
24. R.E. Lyon, U. Sorathia, A.J. Foden, P.N. Balaguru, M. Davidovics, and J. Davidovits, "Fire-Resistant Aluminosilicate Composites," *Fire and Materials*, 21: 67-73, 1997.
25. A.M. Kanury, Introduction to Combustion Phenomena, New York, Gordon and Breach Science Publishers, 1977.
26. I. Glassman, Combustion, 3rd ed., New York, Academic Press, 1996, pp. 285-321.
27. S.R. Turns, An Introduction to Combustion—Concepts and Applications, New York, McGraw-Hill, 1996.
28. R.A. Strehlow, Combustion Fundamentals, New York, McGraw-Hill, 1984.
29. R.M. Aseeva and G.E. Zaikov, Combustion of Polymer Materials, New York, Hanser, 1985.
30. C.F. Cullis and M.M. Hirschler, The Combustion of Organic Polymers, Oxford, England, Clarendon Press, 1981.
31. The SFPE Handbook of Fire Protection Engineering, 2nd ed., Boston, MA, Society of Fire Protection Engineers, 1995, Section 2, Fire Dynamics.
32. D. Drysdale, An Introduction to Fire Dynamics, New York, John Wiley & Sons, 1985.

33. M. Lewin, S.M. Atlas, and E.M. Pearce (eds.), Flame-Retardant Polymeric Materials, New York, Plenum Press, 1975.
34. The SFPE Handbook of Fire Protection Engineering, 2nd ed., Boston, MA, Society of Fire Protection Engineers, 1995, Section 3, Hazard Calculations.
35. V. Babrauskas and S.J. Grayson (eds.), Heat Release in Fires, New York, Elsevier Applied Science, 1992.
36. W. Parker and R. Filipczak, "Modelling the Heat Release Rate of Aircraft Cabin Panels in the Cone and OSU Calorimeters," *Fire and Materials*, 19: 55-59, 1995.
37. C. Di Blasi, "Analysis of Convection and Secondary Reaction Effects Within the Porous Solid Fuels Undergoing Pyrolysis," *Combustion Science and Technology*, 90: 315-340, 1993.
38. I.S. Wichman and A. Atreya, "A Simplified Model for the Pyrolysis of Charring Materials," *Combustion and Flame*, 68: 231-247, 1987.
39. A. Bucsi and J. Rychly, "A Theoretical Approach to Understanding the Connection Between Ignitability and Flammability Parameters of Organic Polymers," *Polymer Degradation and Stability*, 38: 33-40, 1992.
40. B. Moghtaderi, V. Novozhilov, D. Fletcher, and J.H. Kent, "An Integral Model for the Transient Pyrolysis of Solid Materials," *Fire and Materials*, 21: 7-16, 1997.
41. J.G. Quintiere and N. Iqbal, "An Approximate Integral Model for the Burning Rate of a Thermoplastic-Like Material," *Fire and Materials*, 18: 89-98, 1994.
42. A.M. Kanury, "Flaming Ignition of Solid Fuels," in The SFPE Handbook of Fire Protection Engineering, 2nd Edition, Boston, MA, Society of Fire Protection Engineers, 1995, Chapter 2-13.
43. H.S. Carslaw and J.C. Jaeger, Conduction of Heat in Solids, 2nd ed., Oxford, UK, Clarendon Press, 1976, pp. 50-193.
44. R.E. Lyon, "Fire Safe Aircraft Cabin Materials," in G.L. Nelson (ed.), Fire and Polymers II, ACS Symposium Series 599, Washington, D.C., American Chemical Society, 1995, pp. 618-638.
45. J.G. Quintiere, Principles of Fire Behavior, Albany, NY, Del Mar Publishers, 1998, Chapter 5, Flame Spread.
46. A. Tewarson, "Generation of Heat and Chemical Compounds in Fires," in The SFPE Handbook of Fire Protection Engineering, 2nd ed., Boston, MA, Society of Fire Protection Engineers, 1995, Chapter 4.
47. J.D. Rasbash, "Theory in the Evaluation of Fire Properties of Combustible Materials," *Proceedings of 5th International Fire Protection Seminar, Karlsruhe, September 1976*, pp. 113-130.

48. P.K. Kim, P. Pierini, and R. Wessling, "Thermal and Flammability Properties of Poly(P-Phenylenebenzobisoxazole)," *J. Fire Science*, 11(4): 296-307, 1993.
49. N. Grassie, "Polymer Degradation and the Fire Hazard," *Polymer Degradation and Stability*, 30: 3-12, 1990.
50. J. Green, "Mechanisms for Flame Retardancy and Smoke Suppression—A Review," *J. Fire Sciences*, 14: 426-442, 1996.
51. L.A. Wall, "Pyrolysis of Polymers," in Flammability of Solid Plastics, Volume 7, Fire and Flammability Series, Westport, CT, Technomic Publishers, 1974, pp. 323-352.
52. D.W. Van Krevelen, "Thermal Decomposition," in Properties of Polymers, 3rd Edition, New York, Elsevier Scientific, 1990, pp. 641-653.
53. D.W. Van Krevelen, "Some Basic Aspects of Flame Resistance of Polymeric Materials," *Polymer*, 16: 615-620, 1975.
54. P.M. Wolfs, D.W. Van Krevelen, and H.I. Waterman, Brennstoff Chemie, 40: 155-189, 1959.
55. G. Montaudo and C. Puglisi, "Thermal Degradation Mechanisms in Condensation Polymers," in N. Grassie, ed., Developments in Polymer Degradation, Volume 7, New York, Elsevier Applied Science, 1977, pp. 35-80.
56. C.F. Cullis and M.M. Hirschler, The Combustion of Organic Polymers, Oxford, England, Clarendon Press, 1981, Chapter 2, pp. 53-54.
57. F. Shafizadeh, "The Chemistry of Pyrolysis and Combustion," in R. Rowell, ed., The Chemistry of Solid Wood, Washington, D.C., American Chemical Society, 1984.
58. A. Broido and M.A. Nelson, "Char Yield on Pyrolysis of Cellulose," *Combustion and Flame*, 24: 263-268, 1975.
59. C. DiBlasi, "Analysis of Convection and Secondary Reaction Effects Within Porous Solid Fuels Undergoing Pyrolysis," *Combust. Sci. and Tech.*, 90: 315-340, 1993.
60. F. Shafizadeh, "Pyrolysis and Combustion of Cellulosic Materials," *Adv. Carbohydrate Chem.*, 23: 419-425, 1968.
61. I. Milosavljevic and E.M. Suuberg, "Cellulose Thermal Decomposition Kinetics: Global Mass Loss Kinetics," *Ind. Eng. Chem. Res.*, 34(4): 1081-1091, 1995.
62. P.C. Lewellen, W.A. Peters, and J.B. Howard, "Cellulose Pyrolysis Kinetics and Char Formation Mechanism," *Proceedings of 16th Symposium (Int'l.) on Combustion*, The Combustion Institute, 1976, pp. 1471- 1480.
63. J.R. Welker, "The Pyrolysis and Ignition of Cellulosic Materials: A Literature Review," *J. Fire and Flammability*, 1: 12-29, 1970.

64. E.M. Suuberg, I. Milosavljevic, and O.Vahur, "Two-Regime Global Kinetics of Cellulose Pyrolysis: The Role of Tar Evaporation," Proceedings 26th Symposium (Int'l.) on Combustion, The Combustion Institute, 1996, pp. 1515– 1521.
65. I.S. Wichman and A. Atreya, "A Simplified Model for the Pyrolysis of Charring Materials," *Combustion and Flame*, 68: 231- 247, 1987.
66. I.S. Wichman and A.B. Oladipo, "Examination of Three Pyrolytic Reaction Schemes for Cellulose Materials," Proceedings 4th International Symposium on Fire Safety Science, 1994, pp. 313- 323.
67. I.S. Wichman and M. Melaaen, "Modeling the Pyrolysis of Cellulosic Materials," in T. Bridgewater (ed.), Advances in Thermochemical Biomass Conversion, London, Chapman and Hall, 1993.
68. H.L. Friedman, "Kinetics of Thermal Degradation of Char Forming Plastics From Thermogravimetry: Application to a Phenolic Plastic," *J. Polym. Sci., Part C*, 6: 183-195, 1962.
69. J.D. Nam and J.C. Seferis, "Generalized Composite Degradation Kinetics for Polymeric Systems Under Isothermal and Nonisothermal Conditions," *J. Polym. Sci., Part B*, 30: 455- 463, 1992.
70. R.E. Lyon, "Pyrolysis Kinetics of Char-Forming Polymers," *Polymer Degradation and Stability*, 61: 201-210, 1998.
71. R.E. Lyon, Unpublished data, Federal Aviation Administration, 1998.
72. C.P. Fenimore and F.J. Martin, *Combustion and Flame*, 10: 135–142, 1966.
73. D.W. Van Krevelen, Properties of Polymers, New York, Elsevier Scientific, 1976.
74. R.E. Lyon, "An Integral Method of Nonisothermal Kinetic Analysis," *Thermochemica Acta* 297: 117-124, 1997.
75. J.E.J. Stags, "Modeling Thermal Degradation of Polymers Using Single-Step First-Order Kinetics," *Fire Safety Journal*, 32: 17-34, 1999.
76. N. Grassie and A. Scotney, "Activation Energies for the Thermal Degradation of Polymers," in J. Brandrup and E.H. Immergut (eds.), Polymer Handbook, 2nd ed., New York, Wiley Interscience, 1975, pp. 467-471.
77. N. Grassie, "Products of Thermal Degradation of Polymers," in J. Brandrup and E.H. Immergut (eds.), Polymer Handbook, 3rd ed., New York, Wiley Interscience, 1989, pp. 365-397.
78. S. Glasstone, K.J. Laidler, and H. Eyring, The Theory of Rate Processes, New York, McGraw-Hill, 1941, pp. 25-27, 191-193.
79. S.W. Benson, Thermochemical Kinetics, New York, Wiley, 1968, pp. 13, 55-66.

80. N. Koga and J. Sestak, "Kinetic Compensation Effect as a Mathematical Consequence of the Exponential Rate Constant," *Thermochimica Acta* 182: 201-208, 1991.
81. L. Reich and S.S. Stivala, Elements of Polymer Degradation, New York, McGraw-Hill, 1971, Chapter 2.
82. A.K. Burnham and R.L. Braun, "Global Kinetic Analysis of Complex Mixtures," *Energy and Fuels* (in press), 1999.
83. F.D. Rossini (ed.), Experimental Thermochemistry, New York, Interscience, 1956.
84. J. Bicerano, Prediction of Polymer Properties, 2nd ed., New York, Marcel-Dekker, Inc., 1996, Chapter 16, pp. 420-437.
85. D.W. Van Krevelen, "Transport of Thermal Energy," in Properties of Polymers, 3rd ed. New York, Elsevier Scientific, 1990, pp. 525-533.
86. W.J. Dunn and A.J. Hopfinger, "3D QSAR of Flexible Molecules Using Tensor Representation," *Perspectives in Drug Discovery and Design*, 12: 167-182, 1998.
87. C.D.P. Klein and A.J. Hopfinger, "Pharmacological Activity and Membrane Interactions of Antiarrhythmics: 4D-QSAR/QSPR Analysis," *Pharmaceutical Research*, 15(2): 303-311, 1998.
88. M.R. Nyden and J.W. Gilman, "Molecular Dynamics Simulations of the Thermal Degradation of Nano-Confined Polypropylene," *Computational and Theoretical Polymer Science*, 7(3): 191-198, 1998.
89. P.A. Hubbard, W.J. Brittain, W.L. Mattice, and D.J. Brunelle, "Ring-Size Distribution in the Depolymerization of Poly(Butyleneterephthalate)," *Macromolecules*, 31(5): 1518-1522, 1998.
90. R.E. Lyon, unpublished data, Federal Aviation Administration, William J. Hughes Technical Center, Atlantic City International Airport, NJ, 1998.
91. D.W. Van Krevelen, "Char Formation," in Properties of Polymers, 3rd ed., New York, Elsevier Scientific, 1990, pp. 649-652.
92. D.W. Van Krevelen, "Some Basic Aspects of Flame Resistance of Polymeric Materials," *Polymer*, 16: 615-620, 1975.
93. W.W. Wendtlandt, Thermal Methods of Analysis, 2nd ed., New York, John Wiley & Sons, 1974, Chapter II, Thermogravimetry.
94. C.P. Fenimore and F.J. Martin, Combustion and Flame, 10: 135-142, 1966.
95. Flammability Data, *Plastics Digest* 17(1), Englewood, CO, D.A.T.A. Business Publishing, 1996, pp. 773-889.
96. "Standard Test Method for Measuring the Minimum Oxygen Concentration to Support Candle-Like Combustion of Plastics (Oxygen Index)," ASTM 2863, in ASTM Fire Test

- Standards, 3rd ed., Philadelphia, PA, American Society for Testing of Materials, 1990, pp. 278-282.
97. "Flammability of Plastic Materials," Northbrook, IL, Underwriters Laboratories Inc., 1991, UL 94 Section 2 (Horizontal: HB) and Section 3 (Vertical: V-0/1/2).
 98. P.A. Staniland, "Molecular Design of High Temperature Polymers," in Hatada, Kitayama, and Vogl (eds.), Macromolecular Design of Polymeric Materials, New York, Marcell Dekker, 1997, pp. 509-521.
 99. G.C. Tesoro, "Fire Resistance of Engineering Thermoplastics," in G. Nelson (ed.), Fire and Polymers: Hazards Identification and Prevention, ACS Symposium Series 425, Washington, D.C., American Chemical Society, 1990, Chapter 16.
 100. C.P. Fenimore, "Candle-Type Test for Flammability of Polymers," in M. Lewin et al. (eds.), Flame Retardant Polymeric Materials, New York, Plenum Press, 1975, Chapter 9.
 101. A. Tewarson, J.L. Lee, and R.F. Pion, "The Influence of Oxygen Concentration on Fuel Parameters for Fire Modeling," Proceedings 18th Symposium (International) on Combustion, The Combustion Institute, Pittsburgh, PA, 1981, pp. 563-570.
 102. J.D. Nam and J.C. Seferis, "Generalized Composite Degradation Kinetics for Polymeric Systems Under Isothermal and Nonisothermal Conditions," *J. Polym. Sci., Part B, Polymer Physics*, 30: 455-463, 1992.
 103. M. Day, J.D. Cooney, and D.M. Wiles, "A Kinetic Study of the Thermal Decomposition of Poly(Aryl-Ether-Ether-Ketone in nitrogen)," *Polym. Eng. & Sci.*, 29: 19-22, 1989.
 104. N. Grassie and A. Scotney, "Activation Energies for the Thermal Degradation of Polymers," in J. Brandrup and E.H. Immergut (eds.), Polymer Handbook, 2nd ed., New York, Wiley Interscience, 1975, pp. 467-471.
 105. K. Kishore and V.R. Pai Verneker, "Correlation Between Heats of Depolymerization and Activation Energies in the Degradation of Polymers," *J. Polym. Sci., Polymer Letters*, 14: 7761-765, 1976.
 106. N. Grassie, "Products of Thermal Degradation of Polymers," in J. Brandrup and E.H. Immergut (eds.), Polymer Handbook, 3rd ed., New York, Wiley Interscience, 1989, pp. 365-397.
 107. N. Grassie and A. Scotney, "Activation Energies for the Thermal Degradation of Polymers," in J. Brandrup and E.H. Immergut (eds.), Polymer Handbook, 2nd ed., II-467, Wiley Interscience, NY, 1975.
 108. F. Li, L. Huang, Y. Shi, X. Jin, Z. Wu, Z. Shen, K. Chuang, R.E. Lyon, F.W. Harris, and S.Z.D. Cheng, "Thermal Degradation Mechanism and Mechanical Properties of Two High Performance Aromatic Polyimide Fibers," *J. Macromol. Sci.*, B38: 107-122, 1999.
 109. A. Factor, "Char Formation in Aromatic Engineering Polymers," in G. Nelson, ed., Fire and Polymers: Hazards Identification and Prevention, ACS Symposium Series 425, Washington, D.C., American Chemical Society, 1990, pp. 274-287.

110. R.E. Lyon, S. Hackett, and R.N. Walters, "Heats of Combustion of High Temperature Polymers," Federal Aviation Administration Technical Note DOT/FAA/AR-TN97/8, September 1998.
111. ASTM D2382-88, "Standard Test Method for Heat of Combustion of Hydrocarbon Fuels by Bomb Calorimeter (High Precision Method)," in ASTM Fire Test Standards, 3rd ed., Philadelphia, PA, American Society for Testing of Materials, 1990, pp. 230-238.
112. W. Thornton, "The Role of Oxygen to the Heat of Combustion of Organic Compounds," *Philosophical Magazine and J. of Science*, 33: 196-205, 1917.
113. C. Hugget, "Estimation of Rate of Heat Release by Means of Oxygen Consumption Measurements," *Fire and Materials*, 4 (2): 61-65, 1980.
114. M. Janssens and W.J. Parker, "Oxygen Consumption Calorimetry," in V. Babrauskas and S.J. Grayson (eds.), Heat Release in Fires, London, Elsevier Applied Science, 1992, pp. 31-59.
115. V. Babrauskas, "Heat of Combustion and Potential Heat," in V. Babrauskas and S.J. Grayson (eds.), Heat Release in Fires, London, Elsevier Applied Science, 1992, pp. 207-223.
116. W. Wunderlich, "Physical Constants of Poly(Methyl Methacrylate)," in J. Brandrup and E.H. Immergut (eds.), Polymer Handbook, 3rd edition, New York, John Wiley & Sons, 1989, pp. 77-88.
117. D.W. Van Krevlen, "Thermochemical Properties," in Properties of Polymers, 3rd Edition, New York, Elsevier Scientific, 1990, pp. 629-639.
118. J. Green, "Mechanisms for Flame Retardancy and Smoke Suppression-A Review," *J. Fire Sciences*, 14: 427-442, 1996.
119. B.T. Rhodes and J.G. Quintiere, "Burning Rate and Flame Heat Flux for PMMA in a Cone Calorimeter," *Fire Safety J.*, 26: 221-233, 1966.
120. M.M. Hirschler, "Heat Release From Plastic Materials," in V. Babrauskas and S. Grayson (eds.), Heat Release in Fires, New York, Elsevier Applied Science, 1992, pp. 375-442.
121. S. Gandhi, R.N. Walters, and R.E. Lyon, "Heat Release Rates of Engineering Polymers," *Proceedings Fire and Materials Conference*, San Antonio, TX, February 1999.
122. ASTM E 1354-90, "Standard Test Method for Heat and Visible Smoke Release Rates for Materials and Products Using an Oxygen Consumption Calorimeter," in ASTM Fire Test Standards, 3rd edition, Philadelphia, PA, American Society for Testing of Materials, 1990, pp. 803-817.
123. B. Wunderlich, "The Basis of Thermal Analysis," in E. Turi (ed.), Thermal Characterization of Polymeric Materials, New York, Academic Press, Inc., 1981, pp. 91-234.
124. A.K. Burnham and R.L. Braun, "Kinetics of Polymer Decomposition," Report UCID-21293, University of California, Lawrence Livermore National Laboratory, December 1987.